



**HAL**  
open science

# Benthic macrofaunal bioturbation activities from shelf to deep basin in spring to summer transition in the Arctic Ocean

Barbara Oleszczuk, Emma Michaud, Nathalie Morata, Paul Renaud, Monika Kędra

## ► To cite this version:

Barbara Oleszczuk, Emma Michaud, Nathalie Morata, Paul Renaud, Monika Kędra. Benthic macrofaunal bioturbation activities from shelf to deep basin in spring to summer transition in the Arctic Ocean. *Marine Environmental Research*, 2019, 150, pp.104746. 10.1016/j.marenvres.2019.06.008 . hal-02406957

**HAL Id: hal-02406957**

**<https://hal.science/hal-02406957>**

Submitted on 17 Jun 2020

**HAL** is a multi-disciplinary open access archive for the deposit and dissemination of scientific research documents, whether they are published or not. The documents may come from teaching and research institutions in France or abroad, or from public or private research centers.

L'archive ouverte pluridisciplinaire **HAL**, est destinée au dépôt et à la diffusion de documents scientifiques de niveau recherche, publiés ou non, émanant des établissements d'enseignement et de recherche français ou étrangers, des laboratoires publics ou privés.

---

## Benthic macrofaunal bioturbation activities from shelf to deep basin in spring to summer transition in the Arctic Ocean

Oleszczuk Barbara <sup>1,\*</sup>, Michaud Emma <sup>2</sup>, Morata Nathalie <sup>2,3</sup>, Renaud Paul E. <sup>3,4</sup>, Kędra Monika <sup>1</sup>

<sup>1</sup> Institute of Oceanology, Polish Academy of Science (IOPAN), Powstańców Warszawy 55, 81-712, Sopot, Poland

<sup>2</sup> Laboratoire des Sciences de L'environnement Marin Sciences (LEMAR), UMR 6539 (CNRS/UBO/IRD/Ifremer), Institut Universitaire Européen de la Mer, rue Dumont d'Urville, 29280, Plouzané, France

<sup>3</sup> Akvaplan-niva, Fram Centre for Climate and the Environment, Tromsø, Norway

<sup>4</sup> The University Centre in Svalbard, Longyearbyen, Norway

\* Corresponding author : Barbara Oleszczuk, email address : [oleszczuk@iopan.gda.pl](mailto:oleszczuk@iopan.gda.pl)

---

### Abstract :

The aim of this study was to assess bioturbation rates in relation to macrozoobenthos and environmental variables in the Svalbard fjords, Barents Sea and Nansen Basin during spring to summer transition. The results showed differences in benthic community structure across sampled area in relation to sediment type and phytopigment content. Fjords, Barents Sea and the shallow parts of Nansen Basin (<400 m) were characterized by high functional groups diversity, and by biodiffusive and non-local rates ranging from 0.05 to 1.75 cm<sup>-2</sup> y<sup>-1</sup> and from 0.2 to 3.2 y<sup>-1</sup>, respectively. The deeper parts of Nansen Basin, dominated by conveyors species, showed only non-local transport rates (0.1–1 y<sup>-1</sup>). Both coefficients intensity varied with benthic biomass. Non-local transport increased with species richness and density and at stations with mud enriched by fresh phytopigments, whereas biodiffusion varied with sediment type and organic matter quantity. This study quantified for the first time the two modes of sediment mixing in the Arctic, each of which being driven by different environmental and biological situations.

### Highlights

► This is the first complex report on bioturbation in spring to summer transition conducted over a large depth gradient in the Arctic Ocean. ► Benthic community structure and related biodiffusion and non-local transport varied in Svalbard fjords, Barents Sea and Nansen Basin. ► Changes in environmental conditions, and related changes in quality and quantity of available organic matter, had impact on benthic communities and bioturbation. ► Large inputs of fresh OM to the seabed can trigger bioturbation activities.

**Keywords** : non-local transport, biodiffusive transport, macrozoobenthos, spring season, sea ice cover, Arctic Ocean

## 44 **1. Introduction**

45  
46 The structure and functioning of benthic communities depend on the quality and quantity  
47 of organic matter (OM) export fluxes to the sea floor and this dependence increases with  
48 increasing depth. Shallow Arctic shelves benthos is often fueled by high OM fluxes to the sea  
49 floor due to tight pelagic-benthic coupling (e.g. Grebmeier et al., 2006; Tamelander et al.,  
50 2008), while deep-sea communities become food-limited due to low amount of OM reaching

51 sea floor (Maiti et al., 2010). The seasons strongly shape the OM fluxes to the sea floor in the  
52 Arctic marine ecosystems. Phytoplankton and ice algae are two principal sources of primary  
53 production (PP) in the Arctic Ocean with ice algae being the first food source available after  
54 polar night (Søreide et al., 2006, 2008; Leu et al., 2010). Although phytoplankton is  
55 quantitatively dominant, ice algal blooms tend to occur earlier in the seasonally ice-covered  
56 Arctic seas and may contribute up to 50–60% of total PP (Gosselin et al., 1997; McMinn et  
57 al., 2010; Fernandez-Mendez et al., 2015; Van Leeuwe et al., 2018). During the spring, PP is  
58 typically greater than zooplankton consumption and thus highest vertical carbon fluxes are  
59 recorded (Andreassen and Wassmann, 1998; Tamelander et al., 2006). Later in the season, the  
60 zooplankton grazing reduces the OM flux but also adds to it by producing fecal pellets, which  
61 helps phytoplankton sink rapidly to the sea bottom (Olli et al., 2002). In fjords and on the  
62 shelf, benthic communities can also be fueled by terrestrial OM carried by rivers and/or  
63 glaciers, mainly during summer (Bourgeois et al., 2016). Benthic organisms act as temporal  
64 couplers in the seasonal systems, since they can consume variable carbon sources over the  
65 different seasons (McMeans et al., 2015), therefore benthic communities reflect rather long  
66 term (months to years) water column production, while the benthic activities reflect short term  
67 (days to weeks) environmental conditions (Morata and Renaud, 2008).

68         Bioturbation occurs when an organism moves through the sediment, constructs and  
69 maintains burrows, and ingests and defecates. This process results in mixing of particles and  
70 solutes within the substratum (Kristensen et al., 2012), and alters sediment structure (e.g.,  
71 grain size distribution; Montserrat et al., 2009), and production, mineralization and  
72 redistribution of OM (Kure and Forbes, 1997). Life habit, motility, and manner of feeding of  
73 infaunal species induce either random particle movement over a short distance (biodiffusion  
74 (Db) hereafter) (Gérino et al., 2007; Meysman et al., 2003) or biologically induced  
75 discontinuous particle transfer between the sediment surface and deeper sediment layers, for

76 example via burrowing or feeding behavior (non-local transport ( $r$ ) hereafter) (Boudreau,  
77 1986; Meysman et al., 2003; Duport et al., 2007; Gogina et al., 2017). According to the mode  
78 of particle mixing, benthic organisms can be classified into five functional groups of sediment  
79 reworking which may include biodiffusion and/or non-local transport: biodiffusers, gallery-  
80 diffusers, upward- and downward-conveyors, and regenerators (François et al., 1997). The  
81 presence and intensity of these bioturbation modes are therefore mediated by fauna  
82 characteristics like biomass, density, burrowing depth or feeding behavior (François et al.,  
83 1999; Gérino et al., 1998; Sandnes et al., 2000; Gilbert et al., 2007; Michaud et al., 2005,  
84 2006; Duport et al., 2007; Aschenbroich et al., 2017). In turn, species composition, nature and  
85 intensity of their effects on sediment mixing depends on temperature (Ouelette et al., 2004;  
86 Duport et al., 2007; Maire et al., 2007), food inputs (Nogaro et al., 2008) and sediment  
87 characteristics (Needham et al., 2011). Changes in species composition and activities, and  
88 therefore in bioturbation mode and/or intensity, are expected to influence biochemical  
89 processes near the sediment-water interface, including carbon cycling. Bioturbation rate can  
90 therefore be influenced by seasonal changes in PP in the above water column and deposited  
91 OM in the seafloor (food bank; Morata et al., 2015).

92         Only a few studies of bioturbation exist in the Arctic Ocean. Teal et al. (2008) created  
93 the database with global bioturbation intensity coefficient ( $Db$ ) and layer depth ( $L$ ), where  
94 they showed that the Arctic, Central Pacific and most tropical regions are missing bioturbation  
95 data. In polar regions, it has been shown that sediment mixing rates were higher through  
96 biological transports in the shallow sediments directly impacted by the OM input along the  
97 marginal ice covered area of the Barents Sea (Maiti et al., 2010) and in the Svalbard fjords  
98 (Konovalov et al., 2010). On the contrary, the deep sediments of the Arctic Ocean were  
99 marked by lower sediment mixing rates in relation to a lower benthic biomass correlated with  
100 lower OM inputs (Clough et al., 1997). Soltwedel et al. (2019), however, did not confirm a

101 higher bioturbation activity in the high productive Marginal Ice Zone (MIZ) in Fram Strait  
102 compared to the less productive ice zone. Seasonal aspects of bioturbation in the Arctic were  
103 preliminarily studied by Morata et al. (2015), whose experiments showed that the bioturbation  
104 activity was positively correlated with fresh food input during the polar night. McClintic et al.  
105 (2008) found no seasonal variation in bioturbation intensity during June and October in West  
106 Antarctic continental shelf which suggests that deposit feeders are able to access food  
107 particles accumulated during high PP periods. Still, our knowledge on benthic communities  
108 responsible for bioturbation processes and their relation to OM inputs in the Arctic Ocean and  
109 adjacent shelves remains limited, particularly during the spring bloom.

110 The main aim of this study was to understand the impacts of differences in  
111 environmental conditions on benthic communities and their bioturbation function during the  
112 spring to summer transition. We focused on the Svalbard area where fjords, shelf and deep  
113 Nansen Basin differ considerably in terms of physical forcing affecting the quality and  
114 quantity of the OM inputs to the seafloor. Sediment reworking rates were quantified in  
115 relation to taxonomic and functional composition of the benthic macrofaunal communities,  
116 and in relation to the environmental variables. This work is the first study on bioturbation  
117 processes conducted in the Arctic Ocean during spring to summer transition time over a large  
118 depth gradient. It will contribute to our understanding of response of macrofauna and their  
119 activity to the quality and quantity of OM in the Arctic seabed.

120

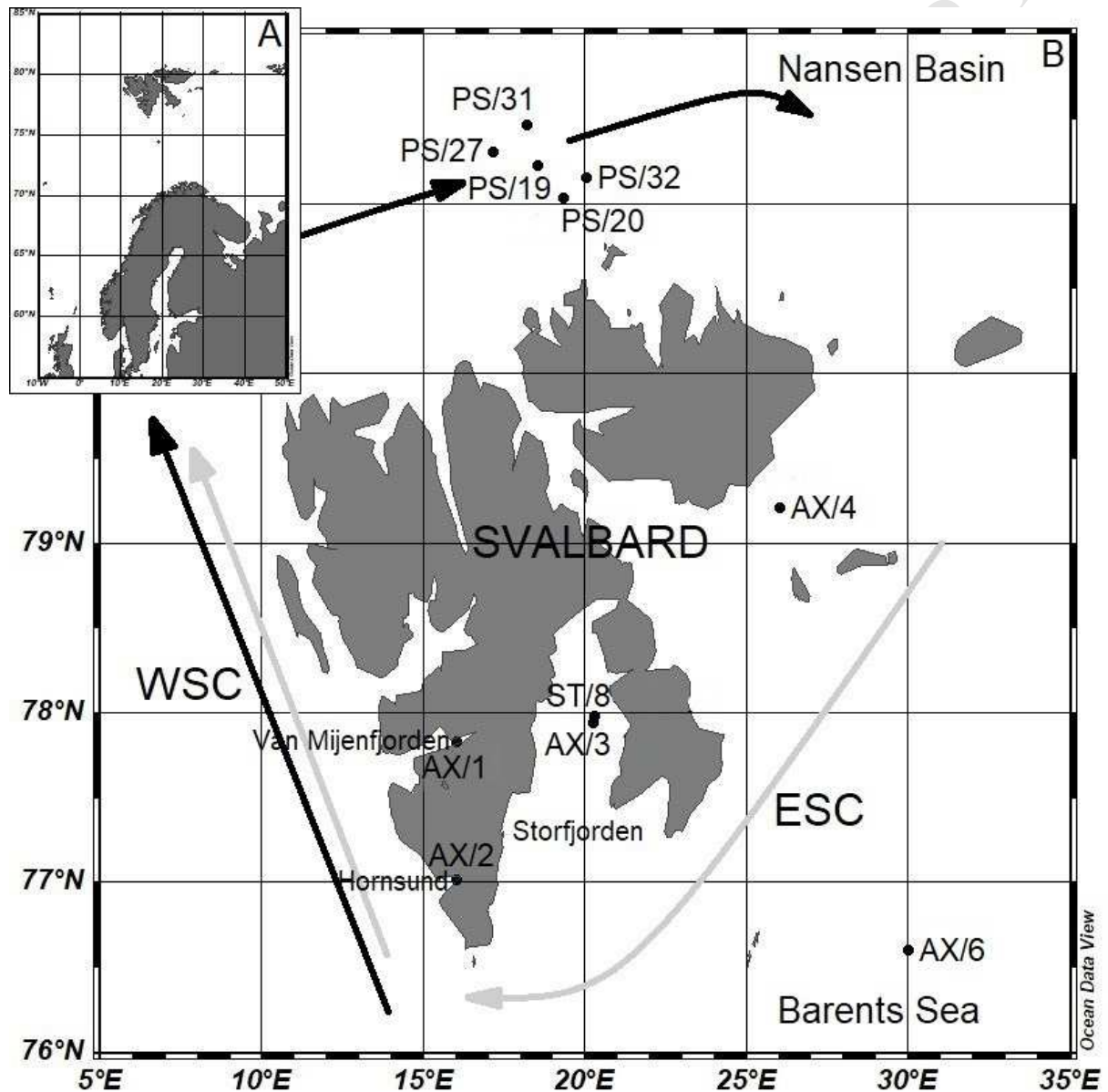
## 121 **2. Material and methods**

122

### 123 *2.1. Study area*

124

125 Sampling was conducted in the Svalbard Archipelago, the Barents Sea and deep Nansen  
 126 Basin north of Svalbard (Fig. 1, Table 1). This area is highly influenced by cold Arctic Water  
 127 coming from the north and warm Atlantic Waters coming from the south, and the relative  
 128 influence of those two water masses varies largely in the study area.  
 129



130  
 131 Fig. 1. Geographical location of the study region (A) and (B) sampling locations during two  
 132 cruises (AX – ARCEX, PS – TRANSSIZ) with two major currents surrounding Svalbard:

- 133 WSC - West Spitsbergen Current, warm Atlantic waters (black) and the ESC – East  
134 Spitsbergen Current, cold Arctic waters (gray) (after Svendsen et al., 2002).

ACCEPTED MANUSCRIPT



135 Table 1. Main characteristics of the sampling stations.

Station	Date	Cruise name	No of cores	Area	Latitude (°N)	Longitude (°E)	Main current	Depth [m]	Bottom Water Salinity	Bottom Water Temperature (°C)
<b>AX/1</b>	19.05.2016	ARCEX	5	Van Mijenfjorden	77.83°	16.47°	ESC	59	34.5	-0.8
<b>AX/2</b>	20.05.2016	ARCEX	5	Hornsund	77.02°	16.45°	ESC	121	34.5	-0.8
<b>AX/3</b>	21.05.2016	ARCEX	5	Storfjorden	77.94°	20.22°	ESC	96	34.5	-0.8
<b>ST/8</b>	15.07.2016	SteP	4	Storfjorden	77.98°	20.28°	ESC	99	34.1	4.5
<b>AX/4</b>	24.05.2016	ARCEX	5	Erik Eriksen Strait	79.21°	26.00°	ESC	217	34.7	0.5
<b>AX/6</b>	25.05.2016	ARCEX	5	Southern Barents Sea	76.60°	30.01°	ESC	278	35.0	2.5
<b>PS/20</b>	30.05.2015	TRANSSIZ	3	Northern Barents Sea	81.04°	19.32°	WSC	170	34.9	0.9
<b>PS/32</b>	06.06.2015	TRANSSIZ	4	Northern Barents Sea	81.16°	20.01°	WSC	312	34.9	2.1
<b>PS/19</b>	29.05.2015	TRANSSIZ	5	Northern Barents Sea	81.23°	18.51°	WSC	471	35.1	1.4
<b>PS/27</b>	01.06.2015	TRANSSIZ	5	Northern Barents Sea	81.31°	17.15°	WSC	842	34.9	0.2
<b>PS/31</b>	04.06.2015	TRANSSIZ	5	Nansen Basin	81.47°	18.17°	WSC	1656	34.9	2.5

136

137

138

139

140 Van Mijenfjorden and Hornsund are located on the west coast of Spitsbergen,  
141 Svalbard. Van Mijenfjorden is a small fjord, nearly closed by an island at its mouth. It is  
142 separated into two basins: the outer (115 m depth) and inner (74 m depth), and by 45 m deep  
143 sill that restricts exchange of water between the fjord and the coastal waters (Skardhamar and  
144 Svendsen, 2010). Hornsund is a large open glacial fjord with eight major tidal glaciers located  
145 in the central and inner parts and large terrestrial inflow (Błaszczuk et al., 2013; Drewnik et  
146 al., 2016). The average depth is 90 m with a maximum of 260 m (Kędra et al., 2013). Strong  
147 gradients in sedimentation, PP and benthic fauna occur along the increasing distance to the  
148 glaciers (Włodarska-Kowalczyk et al., 2013). These high latitude fjords are productive  
149 systems, where PP starts in early spring and continue to late autumn (Fetzer et al., 2002). The  
150 annual PP reaches up to  $216 \text{ g C m}^{-2} \text{ y}^{-1}$  in Hornsund (Smoła et al., 2017). The Barents Sea is  
151 a shelf sea with water depths ranging from 35 m in the Svalbard Bank to up to 400 m or more  
152 in deep depressions and proximal canyon boundaries (Cochrane et al., 2012). The southern  
153 part of the Barents Sea is relatively warm and ice free while its northern parts are seasonally  
154 ice covered, with maximum ice coverage from March to April and minimum ice coverage  
155 generally occurring in September (Vinje, 2009; Ozhigin et al., 2011; Jørgensen et al., 2015). It  
156 is one of the most productive areas in the Arctic Ocean with average PP about  $100 \text{ g C m}^{-2} \text{ y}^{-1}$   
157 and maximum PP reaching over  $300 \text{ g C m}^{-2} \text{ y}^{-1}$  on shallow banks (Sakshaug, 2004).  
158 Storfjorden is located east of Spitsbergen and has a maximum depth of 190 m (Skogseth et al.,  
159 2005). A polynya appears regularly in Storfjorden. It is a very productive area of the Barents  
160 Sea, and its productivity is correlated with the duration of the seasonal sea cover  
161 (Winkelmann and Knies, 2005). In Storfjorden the production of marine organic carbon may  
162 exceed  $300 \text{ mg C cm}^{-2} \text{ kyr}^{-1}$ , while the production of total organic carbon (TOC) may exceed  
163  $500 \text{ mg C cm}^{-2} \text{ kyr}^{-1}$  (Pathirana et al., 2013; Rasmussen and Thomsen, 2014). Nansen Basin,

164 with a maximum depth of 4000 m, is part of the Eurasian basin of the Arctic Ocean. In  
165 general, annual gross PP is within the range of 5–30 g C m<sup>-2</sup> (Codispoti et al., 2013).

166

## 167 2.2. Sampling

168

169 Benthic sampling was conducted during spring cruises of R/V Polarstern PS92 –  
170 TRANSSIZ in May and June 2015, and R/V Helmer Hanssen – ARCEX in May 2016 (Table  
171 1). Samples were collected at 10 stations located along the depth gradient, from Svalbard  
172 fjord (depth: 59 – 121 m), through the Barents shelf and slope (from 170 to 842 m) to the  
173 deep Nansen Basin (max. depth: 1656 m) (Fig. 1). Almost all stations north of Svalbard (P32,  
174 PS/19, PS/27 and PS/31) were sea ice covered during sampling, except PS/20 station. One  
175 station in Storfjorden (AX/3) was revisited in July 2016 during the cruise of R/V L'Atalante –  
176 STeP 2016 (ST/8).

177 At each station the bottom water temperature and salinity were determined by the  
178 shipboard Conductivity Temperature Density (CTD) rosette. Bottom-water samples were  
179 collected using Niskin bottles attached to a CTD and were filtered on pre-combusted  
180 Whatman GF/F glass microfiber filters in triplicate and frozen at -20 °C for later analyses of  
181 bottom water organic carbon (BW C<sub>org</sub>), total nitrogen (BW N<sub>tot</sub>), δ<sup>13</sup>C (BW δ<sup>13</sup>C), δ<sup>15</sup>N (BW  
182 δ<sup>15</sup>N), and C/N ratio (BW C/N).

183 Sediment samples were collected with a box corer of 0.25 m<sup>2</sup> sampling area. The  
184 overlying water from box corer was gently removed from sediment surface and push-cores  
185 samples (12 cm Ø and 20 cm deep, 113.0940 cm<sup>2</sup> surface layer) were collected. The top 2 cm  
186 sediment of the core was sampled for biogeochemical variables (grain size, chlorophyll *a* (Chl  
187 *a*) and phaeopigments (Phaeo), organic matter (SOM), organic carbon (Sed C<sub>org</sub>) and total

188 nitrogen (Sed  $N_{\text{tot}}$ ). Samples were frozen in  $-20\text{ }^{\circ}\text{C}$  and transported to the laboratory for  
189 analysis.

190 Additional sediment cores were taken from the box corer for bioturbation experiments  
191 following procedures described by Morata et al. (2015). Sediment cores (3 to 5 per station,  
192 Table 1) were kept in dark cold room on board (i.e., temperature at  $2\text{ }^{\circ}\text{C}$ , the average between  
193  $-0.8\text{ }^{\circ}\text{C}$  and  $4.5\text{ }^{\circ}\text{C}$  being the range of temperatures observed in the bottom waters, Table 1).

194 Fluorescent luminophores (5 g;  $90\text{--}120\text{ }\mu\text{m}$  diameter) were homogeneously added to  
195 the overlying water and gradually spread on the sediment surface of each core without  
196 disturbing the resident infauna. Cores were then filled with bottom water and aerated by  
197 bubbling to keep the overlying water saturated with oxygen. Overlying water was renewed  
198 every four days. Sediment cores were incubated in those conditions for 10 days which is the  
199 minimum time to enable the characterization of the different transport modes. Incubation time  
200 that exceeds 15 days increases the probability of complete homogenization of the sedimentary  
201 column, and may thus prevent the differentiation of transport modes (François et al., 1997).  
202 This choice of 10 days for duration of experiment was a compromise between the response  
203 that we were expecting from the benthic communities and the available time on board to  
204 process the experiments.

205 After this time of incubation in stable conditions the surface water was carefully  
206 removed and cores were sliced horizontally in 0.5 cm layers from 0 to 2 cm depth, and in 1  
207 cm layers between 2 and 10 cm depth. In total, 12 samples were taken, and each sediment  
208 layer was homogenized. A subsample of each sediment layer was directly frozen ( $-20\text{ }^{\circ}\text{C}$ ) and  
209 used for bioturbation analyses. The remaining sediment of each core samples were sieved  
210 onboard through 0.5 mm sieve for benthic community structure analysis, and fixed with 10 %  
211 buffered formaldehyde.

212

213 2.3. *Biogeochemical environmental analyses*

214

215 Sediments for grain size analysis were freeze-dried at -70 °C, homogenized and dry  
216 sieved into coarse-grained fractions (>0.250 mm) and fine-grained (<0.250 mm). For the fine  
217 fraction, analyses were performed using a Malvern Mastersizer 2000 laser particle analyzer  
218 and presented as volume percent. Mean grain size parameters were calculated using the  
219 geometric method of moments in the program GRADISTAT 8.0 (Blott and Pye, 2001).

220 Pigment concentrations were analyzed fluorometrically following methods described  
221 in Holm-Hansen et al. (1965) to determine Chl *a* and Phaeo concentrations. About 1 g of dried  
222 sediment was extracted with 10 ml of 90 % acetone at 4 °C in the dark. After 24 h, sediment  
223 was then centrifuged (3000 rpm for 2 min), and analysed using a Turner Designs AU-10  
224 fluorometer before and after acidification with 100 µl 0.3 M HCl.

225 For sediment and bottom water biogeochemical parameters analyses, sediments and  
226 filters were dried, homogenized and weighed into silver capsules. For sediment and bottom  
227 water  $\delta^{13}\text{C}$  and  $\delta^{15}\text{N}$ ,  $\text{C}_{\text{org}}$  and  $\text{N}_{\text{tot}}$  analyses, samples were acidified with 2 M HCl to remove  
228 inorganic carbon and dried at 60 °C for 24 h. The analyses were performed on an Elemental  
229 Analyzer Flash EA 1112 Series combined with an Isotopic Ratio Mass Spectrometer IRMS  
230 Delta V Advantage (Thermo Electron Corp., Germany). SOM content was measured as loss  
231 on ignition at 450°C for 4 h (Zaborska et al., 2006). Sed  $\text{C}_{\text{org}}$  content was measured following  
232 the method of Kennedy et al. (2005). About 10 mg of dried sediment was acidified with 50 µl  
233 of 1 N HCl three times. Analyses were run on a Thermo Quest Flash EA 1112 CHN analyzer.

234

235 2.4. *Benthic community analysis*

236

237 In the laboratory, macrofaunal organisms were picked from sediments under a binocular  
238 microscope and identified to the lowest possible taxonomic level. Each taxon was counted,  
239 weighed (g wet weight) and transferred to 70 % ethanol. Mobility and feeding (WoRMS  
240 Editorial Board, 2019), and burrowing behavior (for references see Table 4) were attributed to  
241 each taxon. Benthic fauna was classified into five bioturbation functional groups based on the  
242 type of the sediment mixing: biodiffusers, gallery-diffusers, upward- or downward-conveyors,  
243 and regenerators. Biodiffusers move particles in a random manner in short distances (Gérino,  
244 1992). Gallery-diffusers transport material from the surface sediment layer to deeper by  
245 constructing tubes or tunnels system (François et al., 2002). Upward-conveyors transport  
246 material from depth to the sediment surface and downward-conveyors transport sediment non-  
247 locally to deeper layers (Fisher et al., 1980; Knaust and Bromley, 2012). Regenerators create a  
248 biodiffusion-like process, with large amounts of sediment transported out of the reworked  
249 zone with a strong input to the overlying water column, as well as passive downward  
250 transport of surface sediment to the bottom of the burrow after burrow abandonment (Gardner  
251 et al., 1987; Knaust and Bromley, 2012). Organism density and biomass were evaluated per  
252 taxon, trophic and bioturbation functional group, and in total for each sediment core, and  
253 subsequently converted per  $1 \text{ m}^{-2}$  (area) in order to provide relevant surface values. The  
254 biomass to density (B/D) ratio was calculated per core as a proxy of the mean organism size.

255

## 256 2.5. Bioturbation analyses

257

258 After the sediment cores were sliced, part of the sediment from each sediment layer  
259 was freeze-dried at  $-70 \text{ }^{\circ}\text{C}$ , and homogenized with a mortar and pestle. Three replicates of 0.2  
260 g sediment from each layer were taken and placed on a black box (9.5 cm x 7 cm) under a  
261 constant UV light source ( $350 \pm 370 \text{ nm}$ , Tube UV BLB G5T5 6 W). Images were taken with

262 a digital camera (Nikon digital captor 2.342.016 pixels) with 28  $\mu\text{m}$  per pixel resolution from  
 263 a constant 12 cm from the sediment sample to assure identical acquisition conditions for all  
 264 images (aperture time 1 s; diaphragm aperture f/13, ISO 200). Images were saved in red-  
 265 green-blue (RGB) colour in jpeg format. The images were analysed using an image  
 266 processing toolbox (@mathworks) in order to differentiate luminophores from the background  
 267 sediment by using an appropriate set of RGB threshold levels (Michaud, 2006). Finally, the  
 268 particle size appropriate for each luminophore was selected (6 pixels  $\times$  6 pixels for the  
 269 smallest luminophores), and the pictures were corrected (cleaned) by removing the particle  
 270 sizes smaller and larger than the actual size of the specific luminophore (90–120  $\mu\text{m}$ ). The  
 271 sum of areas (in pixels) of the remaining objects and the number of objects (i.e.,  
 272 luminophores) were calculated for each picture and averaged between the three pictures from  
 273 each sediment layer. Finally, with these abundances for all sediment depths for each core, the  
 274 results were computed as the percentage of detected pixels per depth according to the total  
 275 number of pixels detected per core thus representing the luminophores distribution over depth  
 276 for each sediment core.

277 The reaction diffusion type model used in this paper to describe luminophore  
 278 redistribution following macrofaunal reworking is based on the general diagenetic equation  
 279 (Berner, 1980):

$$280 \frac{\partial Q}{\partial t} = \frac{\partial}{\partial z} \left( Db \frac{\partial Q}{\partial z} \right) + r(Q) \quad (1)$$

281 where Q is the quantity of the tracer (e.g., luminophores), t is the time, z is the depth, Db is  
 282 the apparent biodiffusion coefficient, and r(Q) is the non-continuous displacement of tracer.

283 The term r(Q) is defined as follows:

$$284 r(Q(z, t)) = \begin{cases} \frac{r}{z_2 - z_1} \int_0^{x_1} Q(x, t) dx & \text{if } z \in [z_1; z_2] \\ -rQ(z, t) & \text{if } z \in [0; z_1[ \\ 0 & \text{if } z > z_2 \end{cases} \quad (2a-c)$$

285 where  $z_1$  and  $z_2$  define the upper and lower limits of the tracer redistribution,  $x$  and  $z$  are  
 286 depth variables and  $r$  is the biotransport coefficient that is the percentage of tracer that left the  
 287  $[0; x_1]$  deposit and was redistributed in the  $[z_1; z_2]$  layer. The redistribution of tracer between  
 288  $z_1$  and  $z_2$  and the disappearance of tracer from the  $0-z_1$  layer are, respectively, described by  
 289 Eqs. (2a) and (2b). Eq. (2c) indicates that no tracer movement occurs below  $z_2$ .

290 This displacement term was originally exemplified in a model describing gallery-  
 291 diffusion of macrofaunal reworking (François et al., 2002). This biological reworking process  
 292 describes the diffusive-like mixing of particles in the region of intense burrowing activity and  
 293 the rapid transport of organic and inorganic material from the upper sediment layers to the  
 294 lower regions of reworking (i.e. ‘biotransport’ or “non-local transport”).

295 According to the experimental conditions, the following initial conditions were used:

$$296 \quad Q(z, 0) = \begin{cases} Q_0 & \text{if } z \in [x_1; x_2[ \\ 0 & \text{else} \end{cases} \quad (3)$$

297 where  $[x_1; x_2]$  is the tracer deposit layer. Finally, a zero-flux Neuman boundary condition was  
 298 considered:

$$299 \quad \frac{\partial Q}{\partial z}(0, t) = \lim_{z \rightarrow \infty} \frac{\partial Q}{\partial z}(z, t) = 0 \quad (4)$$

300 The application of this bioturbation model to tracer redistributions, initially started by  
 301 François et al. (1997, 2001) and later revised by Duport et al., (2007), allowed the quantification  
 302 of two particle mixing coefficients: an apparent biodiffusion coefficient  $Db$  and a biotransport  
 303 coefficient  $r$ . The biodiffusion coefficient  $Db$  takes into account the diffusion-like transport  
 304 due to the activity of the organisms. We assume that the actual concentration dependent  
 305 diffusion of tracers is negligible. The biotransport coefficient ( $r$ ) represents a non-local mixing  
 306 pattern associated with a biologically induced transfer of particles from one place to another  
 307 in a discontinuous pattern (i.e. a non-continuous transport; Boudreau, 1986; Meysman et al.,  
 308 2003). Estimates of the parameters  $Db$  and  $r$  were finally obtained by minimizing a weighted  
 309 sum of squared differences between observed and calculated tracer concentrations (François



310 et al., 1999, 2002). For each core, many adjustments between the observed and modelled  
311 profiles are necessary in order to find the minimum weighted sum of squared differences.

312 This model was used with MatLab (@mathworks), thus it gives qualitative data (i.e.,  
313 kind of sediment mixing) and quantitative data (intensity of the sediment mixing) on the  
314 sediment mixing function for the entire benthic community at the sediment-water interface.

315

## 316 2.6. Statistical analysis

317

318 Bray-Curtis similarity matrix, based on square-root transformed data was used for the  
319 multivariate analysis of the macrobenthic community. Principal coordinate analysis (PCO)  
320 was conducted to explore multivariate variability among different sampling stations based on  
321 the (B/D) ratio community composition data matrix. Pearson rank correlation ( $>0.5$ ) vectors  
322 of species B/D with axes were overlaid on the PCO plots to visualize the relationships  
323 between ordination axes and the directions and degrees of variability in the biological  
324 variables. Differences in species composition in samples among the groups of stations were  
325 explored using non-parametric multivariate methods applied to Bray-Curtis dissimilarity  
326 matrix calculated from biomass/density ratio (B/D) (one-way PERMANOVA). Whenever the  
327 significant effect of factor was detected by the main PERMANOVA test, pair-wise tests for  
328 differences between levels of each significant factor was performed. SIMPER procedure  
329 (similarity percentage species contribution) was used to discriminate species responsible for  
330 the differences between sites. In all models, a forward-selection procedure was used to  
331 determine the best combination of predictor variables for explaining the variations in  
332 macrofauna assemblages. The selection criteria chosen for the best-fitting relationship were  
333 based on  $R^2$  values (Anderson et al. 2008). A distance-based linear model (DistLM) was used  
334 to analyse and model the relationships between the macrofaunal community structure and the

335 environmental factors. A distance-based redundancy analysis (dbRDA) was used to visualize  
336 the variability along the two axes that best discriminated groups of samples defined by a priori  
337 assigned groups. Superimposed vectors corresponded to Pearson's correlations ( $>0.5$ ) of  
338 environmental factors with the dbRDA axes. Calculations of the pseudo-F and p values were  
339 based on 999 permutations of the residuals under a reduced model. The significance level for  
340 all the statistical tests was  $p = 0.05$ .

341 The normality of environmental factors and biological factors (non-local and biodiffusion  
342 coefficients, benthic density and biomass) was verified with use of Shapiro-Wilk test  
343 ( $p < 0.05$ ). Since data did not have a normal distribution, Spearman correlations were  
344 calculated to estimate the relationships between faunal community characteristics (Table 8)  
345 and environment (Appendix 1). Differences in benthic density, biomass, non-local and  
346 biodiffusion coefficient were evaluated with the use of the nonparametric Kruskal-Wallis test,  
347 and the Dunn's post-hoc multiple comparison test was applied to identify the differences  
348 among stations groups. Station ST/8, sampled in July, was excluded from those analyses due  
349 to lack of environmental information and because it was sampled during a different season  
350 than the other stations. Additionally, a non-parametric pairwise Mann-Whitney U-test was  
351 performed to compare differences between the spring and summer season in Storfjorden  
352 (AX/3 vs ST/8). All analyses were performed using the PRIMER package v. 7 Clarke and  
353 Gorley, 2006; Anderson et al., 2008) and the Statsoft software STATISTICA v. 9.

354

### 355 **3. Results**

356

#### 357 *3.1. Environmental patterns*

358

359 Bottom water salinity ranged from 34.5 to 35.1 and bottom water temperature ranged  
360 from  $-0.8\text{ }^{\circ}\text{C}$  to  $2.5\text{ }^{\circ}\text{C}$  during our sampling. The lowest BW  $C_{\text{org}}$  concentrations were  
361 measured in Erik Eriksen Strait (AX/4;  $0.1 \pm 0.1\%$ ) and the highest in Storfjorden (AX/3;  $0.6$   
362  $\pm 0.0\%$ ). The BW  $\delta^{13}\text{C}$  values ranged from  $-27.7\text{‰}$  on the slope north of Svalbard (PS/32) to  
363  $-22.2\text{‰}$  in Storfjorden. The lowest BW C/N ratio values were found at the deepest station  
364 (PS/31;  $6.1 \pm 0.0$ ) and the highest values were measured in the southern Barents Sea (AX/6:  
365  $10.3 \pm 1.2$ ) (Table 2). Sandy and muddy sediments dominated in the study area. The lowest  
366 SOM concentrations were measured at station PS/32, on slope ( $2.6\% \pm 0.1$ ) and the highest in  
367 Storfjorden (AX/3;  $6.5\% \pm 0.3$ ). The most depleted sediment  $\delta^{13}\text{C}$  values occurred in fjords  
368 (AX/1:  $-24.2\text{‰}$  and AX/2:  $-25.4\text{‰}$ ) while the most enriched values were found on southern  
369 Barents Sea shelf (AX/6:  $-22.2\text{‰}$ ). The lowest Sed C/N ratio values were found in deep basin  
370 (PS/27:  $7.8 \pm 0.4$ ) and the highest value occurred in Van Mijenfjorden (AX/1:  $18.7 \pm 0.5$ )  
371 (Table 3).

372 Table 2. Bottom water (BW) characteristics for each sampling station:  $C_{org}$ ,  $N_{tot}$ ,  $\delta^{13}C$ ,  $\delta^{15}N$  (in ‰) and C/N values (mean  $\pm$  SD, n=3).

Station	BW $C_{org}$ (%)	BW $N_{tot}$ (%)	BW $\delta^{13}C$ (‰)	BW $\delta^{15}N$ (‰)	BW C/N
AX/1	0.204 $\pm$ 0.017	0.023 $\pm$ 0.002	-24.7 $\pm$ 0.1	5.7 $\pm$ 0.7	10.3 $\pm$ 1.1
AX/2	0.187 $\pm$ 0.005	0.024 $\pm$ 0.001	-24.0 $\pm$ 0.1	3.9 $\pm$ 0.5	8.9 $\pm$ 0.2
AX/3	0.630 $\pm$ 0.037	0.097 $\pm$ 0.005	-22.2 $\pm$ 0.2	4.8 $\pm$ 0.3	7.6 $\pm$ 0.2
ST/8	-	-	-	-	-
AX/4	0.137 $\pm$ 0.047	0.015 $\pm$ 0.003	-24.0 $\pm$ 0.1	5.1 $\pm$ 0.2	10.2 $\pm$ 1.7
AX/6	0.268 $\pm$ 0.013	0.031 $\pm$ 0.005	-24.5 $\pm$ 0.9	5.9 $\pm$ 1.7	10.3 $\pm$ 1.2
PS/20	0.354 $\pm$ 0.017	0.063 $\pm$ 0.001	-23.5 $\pm$ 0.0	1.4 $\pm$ 0.0	6.6 $\pm$ 0.2
PS/32	0.180 $\pm$ 0.002	0.030 $\pm$ 0.001	-27.7 $\pm$ 0.1	1.9 $\pm$ 0.6	7.0 $\pm$ 0.2
PS/19	0.188 $\pm$ 0.014	0.032 $\pm$ 0.001	-24.6 $\pm$ 0.2	2.1 $\pm$ 0.2	6.8 $\pm$ 0.2
PS/27	0.226 $\pm$ 0.007	0.040 $\pm$ 0.001	-22.9 $\pm$ 0.2	2.0 $\pm$ 0.7	6.6 $\pm$ 0.1
PS/31	0.258 $\pm$ 0.013	0.050 $\pm$ 0.002	-23.8 $\pm$ 0.1	2.3 $\pm$ 0.7	6.1 $\pm$ 0.0

373

374

375

376

377

378

379

380

381 Table 3. Sediment variables for each sampling station: sediment type, C<sub>org</sub>, N<sub>tot</sub>,  $\delta^{13}\text{C}$ ,  $\delta^{15}\text{N}$ , OM (in %), C/N, Chl *a* ( $\mu\text{g DW g}^{-1}$ ) and Chl *a*/Phaeo  
 382 values (mean  $\pm$  SD, n=no of cores).

Station	No of cores	Sediment type	Gravel (%)	Sand (%)	Mud (%)	Sed C <sub>org</sub> (%)	Sed N <sub>tot</sub> (%)	Sed $\delta^{13}\text{C}$ (‰)	Sed $\delta^{15}\text{N}$ (‰)	Sed C/N	SOM (%)	Chl <i>a</i> ( $\mu\text{g/g}$ )	Chl <i>a</i> / Phaeo
AX/1	3	Sand	0.0	78.1	21.9	1.9 $\pm$ 0.0	0.1 $\pm$ 0.0	-24.2	4.0	18.7 $\pm$ 0.5	5.1 $\pm$ 0.4	2.3 $\pm$ 0.2	0.5 $\pm$ 0.1
AX/2	3	Sand	1.3	86.8	12.0	1.8 $\pm$ 0.0	0.1 $\pm$ 0.0	-25.4	4.8	18.1 $\pm$ 0.2	4.4 $\pm$ 0.3	1.4 $\pm$ 0.1	0.4 $\pm$ 0.0
AX/3	3	Mud	0.0	40.8	59.2	2.1 $\pm$ 0.0	0.2 $\pm$ 0.0	-22.9	3.6	10.8 $\pm$ 0.1	6.5 $\pm$ 0.3	19.4 $\pm$ 2.6	1.9 $\pm$ 0.4
ST/8	2	-	-	-	-	2.1 $\pm$ 0.0	0.2 $\pm$ 0.0	-	-	11.0 $\pm$ 0.4	7.3 $\pm$ 0.6	21.8 $\pm$ 1.3	51.8 $\pm$ 34.2
AX/4	3	Sand	2.3	66.4	31.2	1.0 $\pm$ 0.0	0.1 $\pm$ 0.0	-23.6	5.3	8.2 $\pm$ 0.2	5.1 $\pm$ 0.6	2.2 $\pm$ 0.3	0.3 $\pm$ 0.0
AX/6	3	Mud	1.3	42.6	56.1	2.1 $\pm$ 0.0	0.3 $\pm$ 0.0	-22.2	4.6	9.9 $\pm$ 0.2	5.7 $\pm$ 0.6	2.6 $\pm$ 0.5	0.4 $\pm$ 0.0
PS/20	2	Sand	7.5	51.3	41.2	0.9 $\pm$ 0.0	0.1 $\pm$ 0.0	-22.8	2.8	8.5 $\pm$ 0.1	4.6 $\pm$ 0.3	7.6 $\pm$ 1.7	1.1 $\pm$ 0.2
PS/32	2	Sand	1.9	76.6	21.5	0.5 $\pm$ 0.1	0.1 $\pm$ 0.0	-22.8	4.0	8.1 $\pm$ 0.2	2.6 $\pm$ 0.1	12.8 $\pm$ 1.6	1.9 $\pm$ 0.4
PS/19	3	Sand	0.1	74.5	25.3	1.6 $\pm$ 0.0	0.2 $\pm$ 0.0	-22.7	4.6	9.5 $\pm$ 0.3	8.3 $\pm$ 0.8	2.9 $\pm$ 0.5	0.4 $\pm$ 0.0
PS/27	3	Sand	6.3	62.3	31.5	0.8 $\pm$ 0.0	0.1 $\pm$ 0.0	-22.9	3.0	7.8 $\pm$ 0.4	3.7 $\pm$ 0.3	2.6 $\pm$ 0.5	0.5 $\pm$ 0.0
PS/31	3	Sand	30.1	46.0	23.9	0.8 $\pm$ 0.1	0.1 $\pm$ 0.0	-23.0	3.9	16.7 $\pm$ 3.8	4.4 $\pm$ 0.1	1.1 $\pm$ 0.4	0.3 $\pm$ 0.0

383

384

385

386

387

388

389 3.2. *Macrobenthic community structure*

390

391 In total, 186 taxa were identified. The number of taxa per station ranged from 9 (AX/2)  
392 to 68 (PS/32) (Table 4). Four burrowing and four sediment-mixing types were recorded. Sub-  
393 surface burrowing, Cirratulidae (biodiffusor) and *Lumbrineris* sp. (gallery diffusor) dominated  
394 in Svalbard fjords in biomass and density, and in Storfjorden in density. The deep burrowing  
395 *Yoldia hyperborea* (conveyor) dominated in biomass at AX/3. Two biodiffusors, the tube  
396 building polychaete *Myriochele heeri* and the deep burrowing bivalve *Astarte borealis*  
397 dominated in Erik Eriksen station (AX/4) in density and biomass respectively. The tube  
398 building *Spiochaetopterus typicus* (conveyor) dominated in terms of density and was second  
399 dominant in biomass in the Southern Barents Sea (AX/6). The sea star *Ctenodiscus* sp.  
400 dominated in biomass at this station. The tube building polychaete, *Maldane glebifex*,  
401 dominated in both density and biomass at the shelf station PS/20. Deep burrowing bivalves  
402 (*Yoldiella lenticula*, *Yoldia hyperborea*) dominated in density at PS/32 while the tube building  
403 polychaete *Galathowenia oculata* dominated in biomass. Burrow-building taxa were mostly  
404 biodiffusors and dominated at all shallow stations. Deep burrowing and tube building taxa  
405 were mostly conveyor bioturbators and dominated at deeper stations (Table 4). Fourteen  
406 mobility-feeding groups were recorded, and sessile and mobile macrofauna dominated at all  
407 stations except from the deepest one (PS/31) where discretely mobile fauna dominated. The  
408 lowest number of functional groups was found in Hornsund (AX/2) where 4 groups (sessile  
409 surface feeders, discretely subsurface feeders, mobile omnivore and mobile subsurface  
410 feeders) occurred. Sessile subsurface feeders dominated at PS/20 (30%) and PS/27 (33%).  
411 Sessile surface feeders were predominant in fjords (AX/1: 52% ; AX/2: 80%), Storfjorden  
412 (AX/3: 35%), in the southern Barents Sea (AX/6: 45%) and on slope (PS/19: 18%). The share  
413 of discretely mobile fauna increased with depth, and discretely mobile surface feeders

414 dominated in the Nansen Basin (PS/31: 44%). The highest number of mobile subsurface  
415 feeders was found on the shelf (PS/32: 23%). The number of mobile taxa was similar for all  
416 stations. The mobile surface fauna dominated in Erik Eriksen Strait (AX/4: 25%) (Fig. 2).

417

418

419

420

421

422

423

424

425

426

427

428

429

430

431

432

433

434

435

436

437

438

439

440

441 Table 4. Functional traits, relative density and biomass of the three dominant taxa for each sampling station. Class: P – Polychaeta, B – Bivalvia,  
 442 An – Anthozoa, As – Asteroidea, O – Ophiuroidea, S – Sipunculidea. Mobility and feeding groups (M/F) are marked by codes: mobility type (D -  
 443 Discretely mobile, M – Mobile, S – Sessile) and feeding type (car - carnivore, omn - omnivore, sub - subsurface feeder, sur - surface feeder, sus -  
 444 suspension feeder). Burrowing depth (BT): 1 – surface burrowing, 2 – subsurface burrowing, 3 – deep burrowing. Tubes (T): “+” – I-shaped  
 445 tube, “-” – no tube. Sediment mixing types (SMix): biodiffusor (B), upward conveyor (UC), gallery diffusor (GD), downward conveyor (DC).

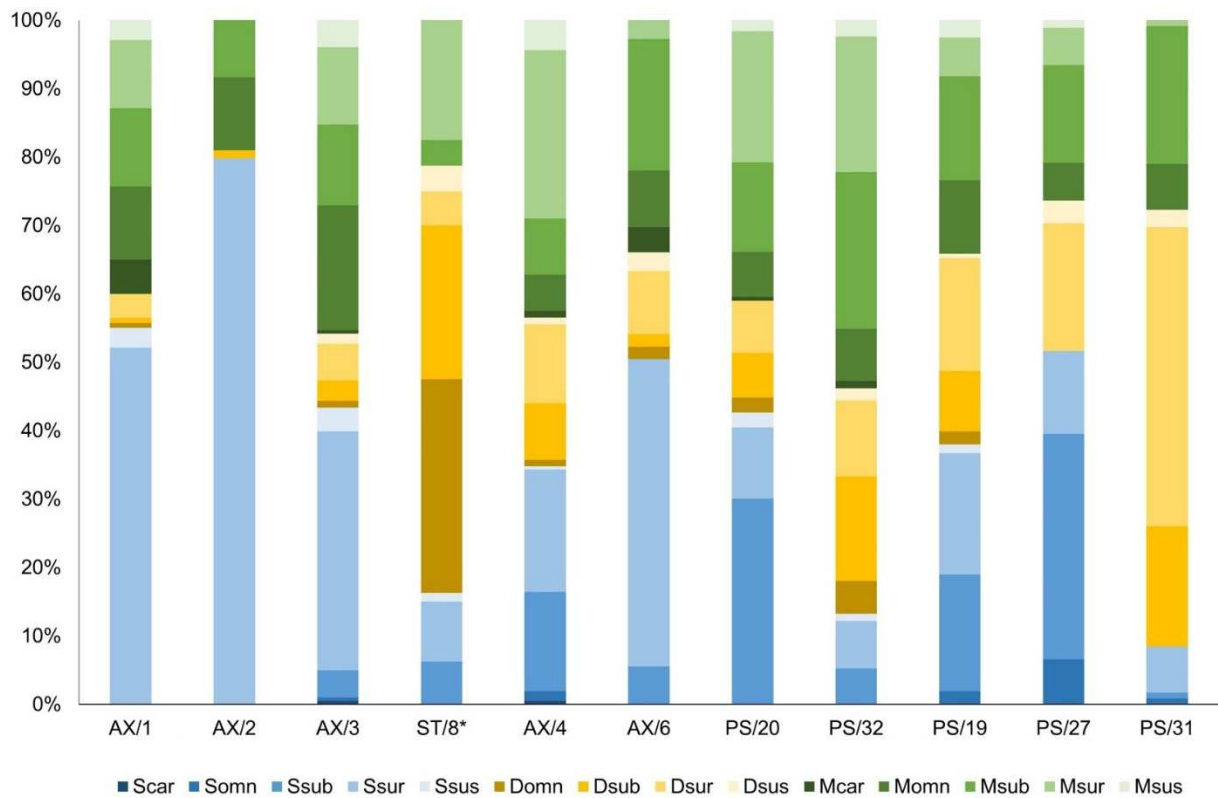
Station	No of taxa	Taxa	Class	M/F	BT	T	SMix	Density %	Taxa	Class	M/F	BT	T	SMix	Biomass %
AX/1	20	Cirratulidae <sup>2</sup>	P	Ssur	2	-	B	41.4	<i>Lumbrineris</i> sp. <sup>6</sup>	P	Momn	2	-	GD	72.1
		<i>Polycirrus arcticus</i> <sup>4,5</sup>	P	Ssur	3	+	DC	7.1	<i>Polycirrus arcticus</i> <sup>4,5</sup>	P	Ssur	3	+	DC	11.5
		<i>Lumbrineris</i> sp. <sup>6</sup>	P	Momn	2	-	GD	6.4	<i>Aglaophamus malmgreni</i> <sup>4</sup>	P	Mcar	2	-	B	10.6
AX/2	9	Cirratulidae <sup>2</sup>	P	Ssur	2	-	B	66.7	Cirratulidae <sup>2</sup>	P	Ssur	2	-	B	49.3
		<i>Polycirrus arcticus</i> <sup>4,5</sup>	P	Ssur	3	+	DC	13.1	<i>Polycirrus arcticus</i> <sup>4,5</sup>	P	Ssur	3	+	DC	36.6
		<i>Lumbrineris</i> sp. <sup>6</sup>	P	Momn	2	-	GD	8.3	<i>Lumbrineris</i> sp. <sup>6</sup>	P	Momn	2	-	GD	8.7
AX/3	34	Cirratulidae <sup>2</sup>	P	Ssur	2	-	B	31.2	<i>Yoldia hyperborea</i> <sup>7</sup>	B	Msub	3	-	C	57.4
		<i>Lumbrineris</i> sp. <sup>6</sup>	P	Momn	2	-	GD	14.1	<i>Maldane sarsi</i> <sup>8</sup>	P	Ssub	3	+	C	12
		<i>Yoldia hyperborea</i> <sup>7</sup>	B	Msub	3	-	C	6.3	<i>Nuculana radiata</i> <sup>4</sup>	B	Msub	3	-	B	11.5
ST/8	29	<i>Lumbrineris</i> sp. <sup>6</sup>	P	Momn	2	-	GD	18.3	<i>Yoldia hyperborea</i> <sup>7</sup>	B	Msub	3	-	C	30.5
		Cirratulidae <sup>2</sup>	P	Ssur	2	-	B	11	<i>Nuculana radiata</i> <sup>4</sup>	B	Msub	3	-	B	27.8
		<i>Eteone longa</i> <sup>9,10</sup>	P	Msub	1	-	GD	7.3	<i>Macoma calcarea</i> <sup>11</sup>	B	Ssur	3	-	B	13.7
AX/4	63	<i>Myriochele heeri</i> <sup>17</sup>	P	Msur	3	+	B	12.1	<i>Astarte borealis</i> <sup>4</sup>	B	Msus	3	-	B	90



		<i>Macoma</i> sp. <sup>1,11</sup>	B	Ssur	3	-	B	11.6	Actinaria <sup>4</sup>	An	Scar	1	-	B	1.8
		<i>Maldane sarsi</i> <sup>8</sup>	P	Ssub	3	+	C	8.2	<i>Yoldiella lenticula</i> <sup>7</sup>	B	Msur	3	-	C	1.5
<b>AX/6</b>	36	<i>Spiochaetopterus typicus</i> <sup>8</sup>	P	Ssur	3	+	C	34.9	<i>Ctenodiscus</i> sp. <sup>20</sup>	As	Msur	1	-	B	47.3
		<i>Macoma</i> sp. <sup>1,11</sup>	B	Ssur	3	-	B	6.4	<i>Spiochaetopterus typicus</i> <sup>8</sup>	P	Ssur	3	+	C	27.3
		<i>Heteromastus</i> sp. <sup>12,13,14</sup>	P	Msub	3	-	C	6.4	<i>Aglaophamus malmgreni</i> <sup>4</sup>	P	Mcar	2	-	B	6.4
<b>PS/20</b>	58	<i>Maldane glebifex</i> <sup>8</sup>	P	Ssub	3	+	C	22.4	<i>Maldane glebifex</i> <sup>8</sup>	P	Ssub	3	+	C	24.5
		<i>Yoldiella lenticula</i> <sup>7</sup>	B	Msur	3	-	C	8.7	<i>Chirimia biceps</i> <sup>8</sup>	P	Ssub	3	+	C	9.4
		<i>Macoma calcarea</i> <sup>11</sup>	B	Ssur	3	-	B	7.1	<i>Nicomache lumbricalis</i> <sup>8</sup>	P	Ssub	3	+	C	9.4
<b>PS/32</b>	68	<i>Yoldiella lenticula</i> <sup>7</sup>	B	Msur	3	-	C	13.8	<i>Galathowenia oculata</i> <sup>3</sup>	P	Msur	2	+	C	7.7
		<i>Yoldia hyperborea</i> <sup>7</sup>	B	Msub	3	-	C	8.7	<i>Ctenodiscus</i> sp. <sup>20</sup>	As	Msur	1	-	B	7.5
		<i>Axinopsida orbiculata</i> <sup>15</sup>	B	Dsub	3	-	C	5.9	<i>Yoldiella lenticula</i> <sup>7</sup>	B	Msur	3	-	C	6.3
<b>PS/19</b>	38	Cirratulidae <sup>2</sup>	P	Ssur	2	-	B	12	<i>Amphiura sundevalli</i> <sup>4</sup>	O	Msus	1	-	B	25.5
		<i>Notoproctus oculus</i> <sup>8</sup>	P	Ssub	3	+	C	10.1	Lumbrineridae <sup>6</sup>	P	Somn	2	-	GD	9.3
		<i>Yoldia hyperborea</i> <sup>7</sup>	B	Msub	3	-	C	8.9	Nemertea <sup>4</sup>	N	Momn	1	-	B	7.1
<b>PS/27</b>	35	<i>Prionospio cirrifera</i> <sup>16</sup>	P	Dsur	2	+	C	13.2	<i>Streblosoma intestinale</i> <sup>4</sup>	P	Dsur	3	+	C	43
		<i>Notoproctus oculus</i> <sup>8</sup>	P	Ssub	3	+	C	13.2	<i>Chone fauveli</i> <sup>3</sup>	P	Ssur	2	+	C	32.6
		<i>Lumbriclymene minor</i> <sup>8</sup>	P	Ssub	3	+	C	8.8	<i>Notoproctus oculus</i> <sup>8</sup>	P	Ssub	3	+	C	4.2
<b>PS/31</b>	19	<i>Levinsenia gracilis</i> <sup>18</sup>	P	Dsur	2	-	C	33.6	<i>Nephasoma lilljeborgi</i> <sup>19</sup>	S	Dsur	3	-	C	28
		Paraonidae <sup>2</sup>	P	Msub	2	-	B	19.3	<i>Levinsenia gracilis</i> <sup>18</sup>	P	Dsur	2	-	C	14.2
		<i>Cirrophorus</i> sp. <sup>2</sup>	P	Dsub	2	-	B	16.8	Paraonidae <sup>2</sup>	P	Msub	2	-	B	11

447 References in superscripts: <sup>1</sup> Gilbert et al. (2007); <sup>2</sup> Gérino et al. (1992, 2007); <sup>3</sup> Fauchald and Jumars (1979); <sup>4</sup> Queirós et al. (2013); <sup>5</sup> Gingras et  
448 al. (2008); <sup>6</sup> Petch (1986); <sup>7</sup> Stead and Thompson (2006); <sup>8</sup> Smith and Shafer (1984); <sup>9</sup> Mazik and Elliott (2000); <sup>10</sup> Mermillod-Blondin et al.  
449 (2003); <sup>11</sup> Michaud et al. (2006); <sup>12</sup> D'Andrea et al. (2004); <sup>13</sup> Mulsow et al. (2002); <sup>14</sup> Quintana et al. (2007); <sup>15</sup> Zanzerl and Dufour (2017); <sup>16</sup>  
450 Bouchet et al. (2009); <sup>17</sup> Duchêne and Rosenberg (2001); <sup>18</sup> Venturini et al. (2011); <sup>19</sup> Shields and Kędra (2009); <sup>20</sup> Shick (1976).

451

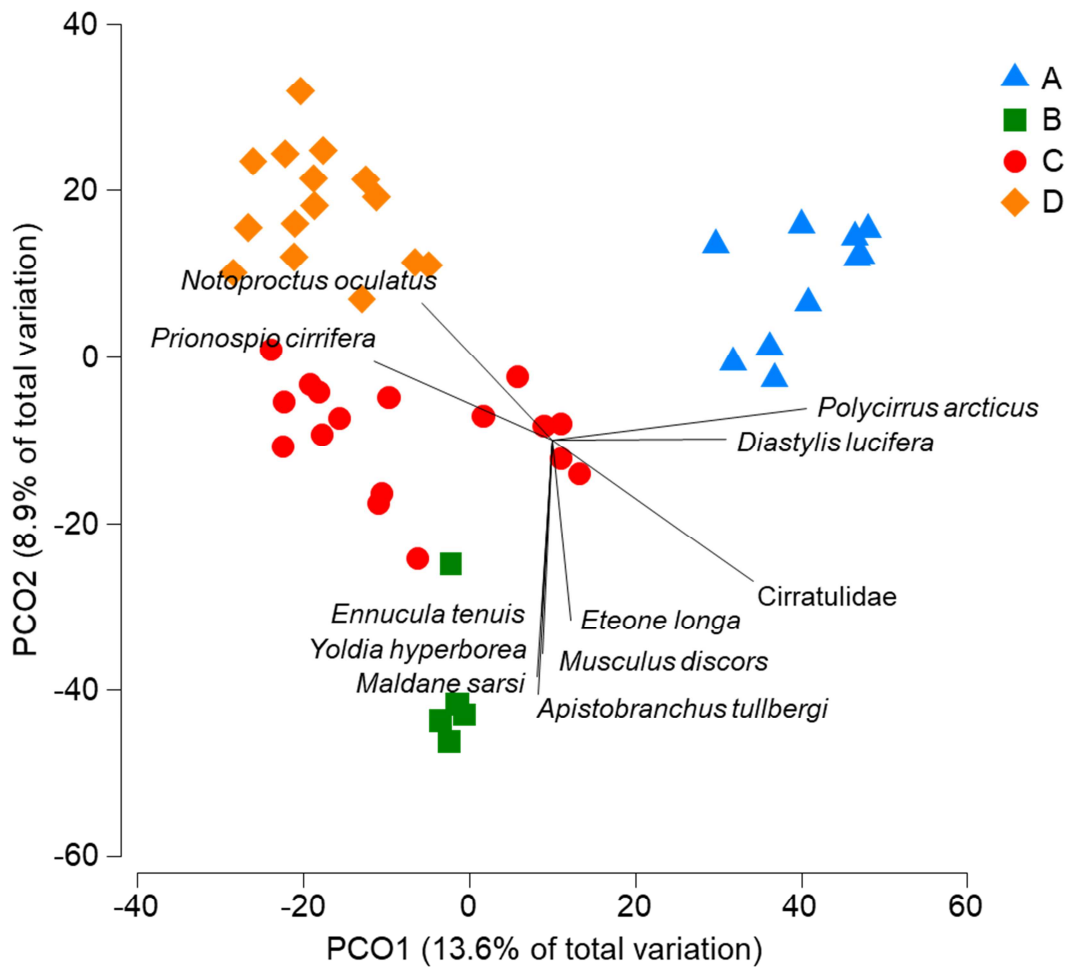


452

453 Fig. 2. Percentages of mobility and feeding groups at different sampling stations. Station ST/8  
 454 marked with \* was sampled in summer season. Functional traits codes: mobility type (D -  
 455 Discretely mobile (yellow), M – Mobile (green), S – Sessile (blue)) and feeding type (car -  
 456 carnivore, omn - omnivore, sub - subsurface feeder, sur - surface feeder, sus - suspension  
 457 feeder).

458 Stations were separated into 4 groups, based on the PCO analysis: A - fjords (Van  
 459 Mijenfjorden: AX/1, Hornsund: AX/2), B - Storfjorden (AX/3), C - Barents Sea shelf (Erik  
 460 Eriksen Strait: AX/4, southern Barents Sea: AX/6, and northern Barents Sea: PS/20, PS/32), D  
 461 - northern Barents Sea, stations deeper than 400m on continental stock: PS/19, PS/27 and  
 462 Nansen Basin: PS/31. PCO explained 22.5% of the variability among sampling stations: the  
 463 first axis explained 13.6% and the second axis 8.9% (Fig. 3). Fjords' communities were  
 464 correlated with presence of polychaete *Polycirrus arcticus* and cumacean *Diastylis lucifera*  
 465 while benthic patterns in Storfjorden were correlated with presence of polychaetes *Maldane*

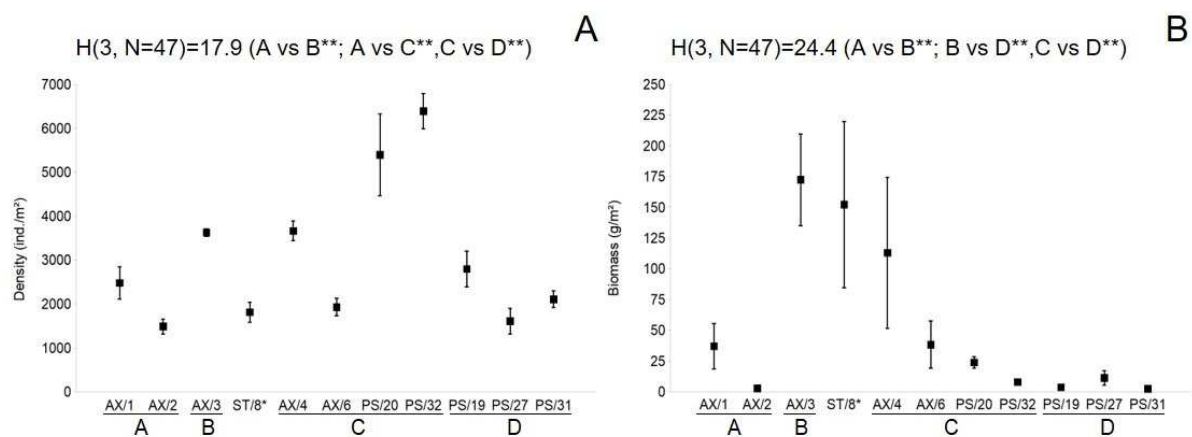
466 *sarsi* and *Apistobranchnus tullbergi*, and bivalves *Musculus discors*, *Ennucula tenuis* and  
 467 *Yoldia hyperborea*. Those correlations were negative for deeper stations where benthic  
 468 communities were mainly correlated with presence of polychaetes *Notoproctus oculatus* and  
 469 *Prionospio cirrifera*. The shelf stations varied the most with less clear patterns for benthic  
 470 communities.



471  
 472 Fig. 3. PCO analysis for macrobenthic communities based on species biomass to density ratio,  
 473 and the Bray-Curtis similarity among four sampling areas: A (Hornsund, Van Mijenfjorden);  
 474 B (Storfjorden); C (Barents Sea shelf); D (northern Barents Sea and Nansen Basin).  
 475 Significantly correlated species with the PCO coordinates ( $r > 0.5$ ) are shown on the plot.

476

477 Polychaeta dominated at all stations. There were significant differences in density  
 478 (Kruskal-Wallis test;  $p < 0.05$ ; significant differences (post hoc test) between group A:B, A:C  
 479 and C:D) (Fig. 4A). Benthic density ranged from  $1485.5 \text{ ind./m}^2 \pm 168.7$  standard error (SE)  
 480 (station AX/2) to  $2475.8 \text{ ind./m}^2 \pm 369.9$  SE (station AX/1) in group A. In group B benthic  
 481 density was  $3625.3 \text{ ind./m}^2 \pm 83.9$  SE (station AX/3). In group C density ranged from  $1927.6$   
 482  $\text{ind./m}^2 \pm 196.5$  SE (station AX/6) to  $6388.5 \text{ ind./m}^2 \pm 399.3$  SE (station PS/32). In group D  
 483 density ranged from  $1609.3 \text{ ind./m}^2 \pm 295.1$  SE (station PS/27) to  $2794.1 \text{ ind./m}^2 \pm 404.8$  SE  
 484 (station PS/19). There were significant differences in biomass among areas (Kruskal-Wallis  
 485 test;  $p < 0.05$ ; significant differences (post hoc test) between group A:B, B:D and C:D) (Fig.  
 486 4B). Benthic biomass ranged from  $2.6 \text{ g wet weight/m}^2 \pm 0.5$  SE (station AX/2) to  $37 \text{ g wet}$   
 487  $\text{weight/m}^2 \pm 18.4$  SE (station AX/1) in group A. In group B benthic biomass was  $172.3 \text{ g wet}$   
 488  $\text{weight/m}^2 \pm 37.3$  SE (station AX/3). In group C biomass ranged from  $7.8 \text{ g wet weight/m}^2 \pm$   
 489  $1.1$  SE (station PS/32) to  $112.9 \text{ g wet weight/m}^2 \pm 61.3$  SE (station AX/4). In group D biomass  
 490 ranged from  $2.2 \text{ g wet weight/m}^2 \pm 0.5$  SE (station PS/31) to  $11.2 \text{ g wet weight/m}^2 \pm 5.7$  SE  
 491 (station PS/27).



492  
 493 Fig. 4. Mean density ( $\text{ind./m}^2$ ) (A) and biomass ( $\text{g/m}^2$ ) (B);  $\pm$  SE, n= no of cores (Table 1) at  
 494 stations sampled in Van Mijenfjorden, Hornsund (group A); Storfjorden (group B); Barents  
 495 Sea shelf (group C); northern Barents Sea and Nansen Basin (group D). Station ST/8 marked

496 with \* was sampled in summer season. Kruskal – Wallis results for differences between  
 497 sampling sites are given; significant test results are marked with \*\* ( $p < 0.05$ ).

498 There were significant differences in the benthic communities structure  
 499 (biomass/density ratio) among different locations (PERMANOVA test Pseudo-F: 5.07,  
 500  $p = 0.001$ ). Significant differences were found for each group (significant pairwise  
 501 comparisons  $p = 0.001$ ); see Table 5 for details.

502

503 Table 5. PERMANOVA results for the multivariate descriptors of benthic communities with  
 504 significant pair-wise comparisons results for different groups.

Benthic parameter	Source of variation	Df	MS	Pseudo-F	P (perm)
Biomass/Density ratio	Gr	3	16606.0	5.07	0.001
	Res	43	3272.8		
	Total	46			

Benthic parameter	Regime	Site	t	Df	P(MC)	P (perm)
Biomass/Density ratio	Groups	A:B	2.886	13	0.001	0.001
		A:C	2.469	25	0.001	0.001
		A:D	2.715	23	0.001	0.001
		B:C	1.874	20	0.001	0.001
		B:D	2.151	18	0.001	0.001
		C:D	1.852	30	0.001	0.001

505

506

507 Benthic taxa that contributed mostly to the groups similarities were: *Polycirrus*  
 508 *arcticus* (44.7 %) in fjords (A), *Yoldia hyperborea* (31.7 %) in Storfjorden (B),  
 509 *Spiochaetopterus typicus* (16.8 %) in the Barents Sea shelf (C) and *Nephasoma diaphanes*  
 510 *diaphanes* (16 %) in the northern Barents Sea and Nansen Basin (D) as revealed by SIMPER  
 511 analysis (Table 6).

512

513 Table 6. SIMPER analysis results based on B/D ratio. Species that contributed more than 5%  
 514 of the average similarity for different sampling stations groups are listed.

Group	Average similarity	Species	Contribution %
A	39.7	<i>Polycirrus arcticus</i>	44.7
		Cirratulidae	28.5
		<i>Lumbrineris</i> sp.	18.7
B	35.9	<i>Yoldia hyperborea</i>	31.7
		<i>Maldane sarsi</i>	31
		<i>Nuculana radiata</i>	9
		<i>Lumbrineris</i> sp.	8.1
		Cirratulidae	5.8
		<i>Spiochaetopterus typicus</i>	16.8
C	12	<i>Lumbrineris</i> sp.	10.7
		<i>Yoldiella lenticula</i>	7.3
		<i>Maldane sarsi</i>	5.6
		<i>Nephasoma diaphanes diaphanes</i>	16
D	14.8	<i>Maldane glebifex</i>	11.7
		<i>Prionospio cirrifera</i>	10.1
		<i>Notoproctus oculatus</i>	9.8
		Nemertea	9.5
		<i>Lumbrineris</i> sp.	6.3
		<i>Byblis minuticornis</i>	5.9

515

516 The results of DistLM analyses showed that salinity explained 10.1% of the variation  
517 observed in the macrofauna community while Sed  $\delta^{13}\text{C}$  (10%) and Sed C/N (9.3%) were next  
518 main contributors. Nine variables were included by the DistLM procedure to construct the  
519 best fitting model, together explaining 46.8% of total variation. However, one of the variables  
520 was not statistically significant (gravel) (Table 7). The most important parameter contributing  
521 to the first axis of the dbRDA plot was Sed C/N and explained 17.2% of fitted variation. It  
522 also positively correlated with fjords' group (A). The most important parameter contributing  
523 to the second axis was sediment Chl *a* and explained 25.7% of fitted flux variation. It was  
524 positively correlated with Storfjords group (B) and most stations in group C (shelf) (Fig. 5).

525

526 Table 7. Results of DistLM procedure for fitting environmental variables to the macrofauna  
527 community data. %Var - percentage of explained variance; %Cum - cumulative percentage  
528 explained by the added variable. Significance level  $p < 0.05$ . Environmental factors: D –  
529 depth, S – salinity, T – temperature, types of sediment (mud, sand, gravel), BW  $\text{C}_{\text{org}}$  – bottom  
530 water  $\text{C}_{\text{org}}$ , BW  $\text{N}_{\text{tot}}$  – bottom water  $\text{N}_{\text{tot}}$ , BW  $\delta^{13}\text{C}$  – bottom water  $\delta^{13}\text{C}$  BW, BW  $\delta^{15}\text{N}$  –

531 bottom water  $\delta^{15}\text{N}$ , BW C/N – bottom water C/N, Sed  $\text{C}_{\text{org}}$  –  $\text{C}_{\text{org}}$  concentration in sediment,  
 532 Sed  $\text{N}_{\text{tot}}$  – sediment  $\text{N}_{\text{tot}}$ , Sed  $\delta^{13}\text{C}$  – sediment  $\delta^{13}\text{C}$ , Sed  $\delta^{15}\text{N}$  – sediment  $\delta^{15}\text{N}$ , Sed C/N –  
 533 sediment C/N, SOM – sediment organic matter, Chl *a* – sediment Chlorophyll *a* and Chl  
 534 *a*/Phaeo – sediment Phaeopigments.

**MARGINAL TESTS**

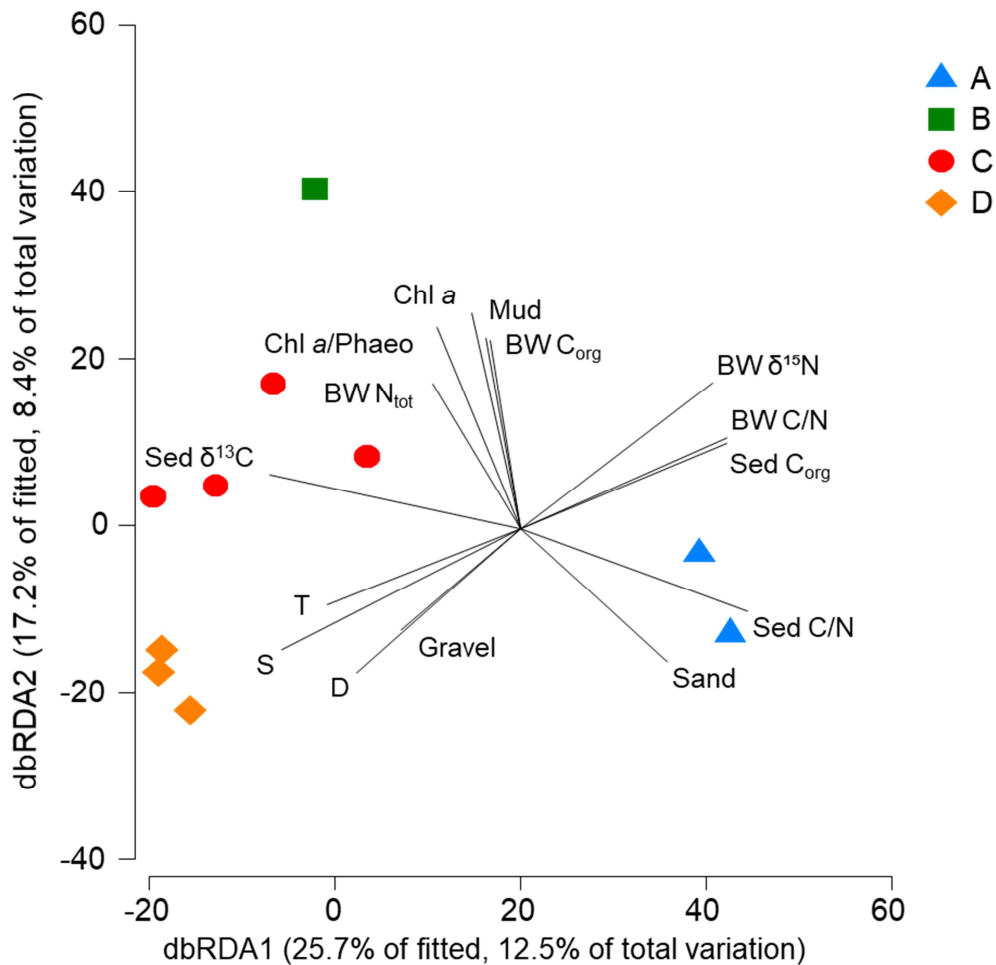
Variable	Pseudo-F	Var%	P
S	5.06	10.1	0.001
Sed $\delta^{13}\text{C}$	5.01	10.0	0.001
Sed C/N	4.59	9.3	0.001
BW C/N	4.31	8.7	0.001
BW $\delta^{15}\text{N}$	4.25	8.6	0.001
Sed $\text{C}_{\text{org}}$	4.11	8.4	0.001
D	3.99	8.1	0.001
T	3.96	8.1	0.001
Chl <i>a</i>	3.66	7.5	0.001
Sand	3.62	7.4	0.001
Mud	3.46	7.1	0.001
Chl <i>a</i> / Phaeo	3.34	6.9	0.001
BW $\text{C}_{\text{org}}$	3.26	6.8	0.001
BW $\text{N}_{\text{tot}}$	3.16	6.6	0.002
Gravel	3.11	6.5	0.001
Sed $\text{N}_{\text{tot}}$	2.43	5.1	0.001
Sed $\delta^{15}\text{N}$	2.09	4.4	0.004
BW $\delta^{13}\text{C}$	2.04	4.3	0.001
SOM	1.56	3.4	0.032

**SEQUENTIAL TESTS**

Variable	R <sup>2</sup>	Pseudo-F	Var%	Cum%	P
D	0.08	3.99	8.1	8.1	0.001
S	0.16	3.98	7.6	15.7	0.001
Sand	0.30	4.06	7.0	22.7	0.001
BW $\delta^{15}\text{N}$	0.44	3.71	5.5	28.2	0.001
BW C/N	0.49	3.70	5.1	33.3	0.001
BW $\delta^{13}\text{C}$	0.38	3.06	4.9	38.1	0.001
T	0.20	2.44	4.5	42.7	0.001
Mud	0.33	2.26	3.8	46.4	0.001
Gravel	0.23	1.29	2.4	48.8	0.127

535





536

537 Fig. 5. Distance-based Redundancy Analysis (dbRDA) plot of the DistLM model visualizing  
 538 the relationships between the environmental parameters and the biomass/density ratio of  
 539 species between four sampling areas: A (Hornsund, Van Mijenfjorden); B (Storfjorden); C  
 540 (Barents Sea shelf); D (northern Barents Sea and Nansen Basin). Environmental variables  
 541 with Pearson rank correlations with dbRDA axes  $> 0.5$  are shown. Environmental factors: D –  
 542 depth, S – salinity, T – temperature, types of sediment (mud, sand, gravel), BW C<sub>org</sub> – bottom  
 543 water C<sub>org</sub>, BW N<sub>tot</sub> – bottom water N<sub>tot</sub>, BW δ<sup>15</sup>N – bottom water δ<sup>15</sup>N, BW C/N – bottom  
 544 water C/N, Sed C<sub>org</sub> – C<sub>org</sub> concentration in sediment, Sed δ<sup>13</sup>C – sediment δ<sup>13</sup>C, Sed C/N –  
 545 sediment C/N, Chl a – sediment Chlorophyll a and Chl a/Phaeo – sediment Phaeopigments.

546

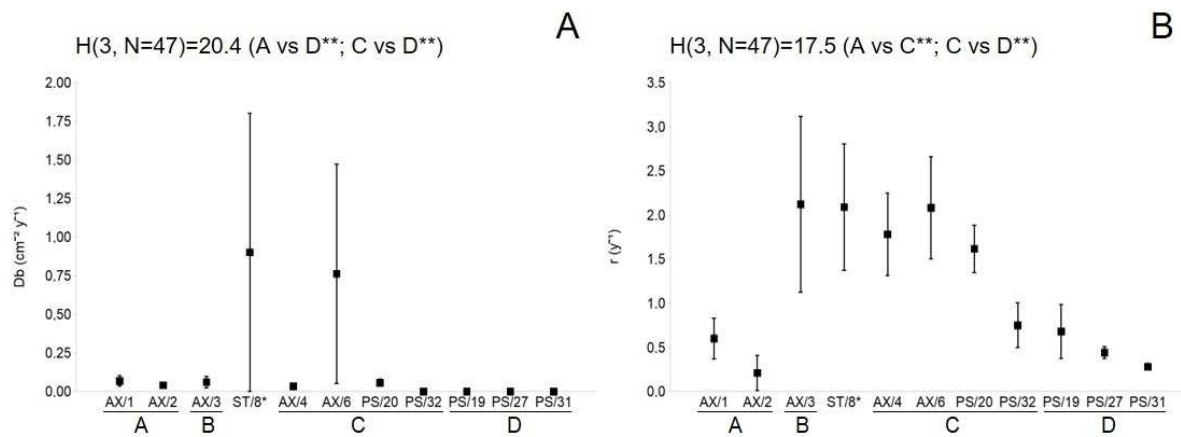
547 *3.3. Bioturbation*

548

549 After 10 days, almost all luminophores (~95%) remained on sediment core surface at all  
550 sampling stations meaning that about 5% of luminophores were transported into sediments.  
551 The fastest decrease was noted at the B group (Storfjorden : AX/3 and ST/8), and at the C  
552 group (Southern Barents Sea station (AX/6) ; Nansen Basin < 400 m (PS/20, PS/32)) where  
553 ~15 to 25% of surface luminophores were buried. While luminophores were still present all  
554 along the sedimentary column in the Storfjorden station, some subsurface peaks of  
555 luminophores were clearly measured below 3 cm in the C group. The lowest decrease of the  
556 luminophores over depth was noted in the A group (Svalbard Fjords AX1/1, AX/2) and in the  
557 D group at deepest station (PS/31) in the Nansen Basin where 92 to 98% of luminophores  
558 remained at surface with slight subsurface peaks of tracers (about: only 0.91 %) between 1 to  
559 3 cm deep .

560 Biodiffusion rates ranged from  $0.04 \text{ cm}^{-2} \text{ y}^{-1} \pm 0.01$  standard error (SE) (station AX/2)  
561 to  $0.07 \text{ cm}^{-2} \text{ y}^{-1} \pm 0.03$  SE (station AX/1) in group A. In group B biodiffusion rates was  $0.06$   
562  $\text{cm}^{-2} \text{ y}^{-1} \pm 0.04$  SE (station AX/3). In group C biodiffusion ranged from 0 (station PS/32) to  
563  $0.76 \text{ cm}^{-2} \text{ y}^{-1} \pm 0.71$  SE (station AX/6). There was no biodiffusive transport in group D. There  
564 were significant differences in biodiffusion among areas (Kruskal-Wallis test;  $p < 0.05$ ;  
565 significant differences (post hoc test) between group A:D and C:D) (Fig. 6A). Non-local  
566 transport rates ranged from  $0.21 \text{ y}^{-1} \pm 0.20$  SE (station AX/2) to  $0.60 \text{ y}^{-1} \pm 0.23$  SE (station  
567 AX/1) in group A. In group B non-local transport rates was  $2.12 \text{ y}^{-1} \pm 1$  SE (station AX/3). In  
568 group C non-local transport rates ranged from  $0.75 \text{ y}^{-1} \pm 0.25$  SE (station PS/32) to  $2.08 \text{ y}^{-1} \pm$   
569  $0.58$  SE (station AX/6). In group D non-local transport rates ranged from  $0.28 \text{ y}^{-1} \pm 0.04$  SE  
570 (station PS/31) to  $0.68 \text{ y}^{-1} \pm 0.31$  SE (station PS/19). There were significant differences in  
571 non-local transport (Kruskal-Wallis test;  $p < 0.05$ ; significant differences (post hoc test)  
572 between group A:C and C:D) (Fig. 6B). Biodiffusive transport values were significantly

573 related with depth, Sed  $C_{org}$  and BW C/N ratio Spearman correlation: -0.6, 0.6 and 0.6,  $p < 0.05$   
 574 respectively). Non-local transport values were significantly related to benthic taxa richness,  
 575 biomass, mud and Sed  $N_{tot}$  (Spearman correlation: 0.5, 0.5, 0.5 and 0.5  $p < 0.05$  respectively)  
 576 (Table 8).



577  
 578 Fig. 6. Mean bioturbation coefficients:  $Db$  - bioturbation (cm<sup>2</sup> y<sup>-1</sup>) (A) and  $r$  – non-local (y<sup>-1</sup>)  
 579 (B);  $\pm$  SE,  $n$ =no of cores (Table 1) at stations sampled in Van Mijenfjorden, Hornsund (group  
 580 A); Storfjorden (group B); Barents Sea shelf (group C); northern Barents Sea and Nansen  
 581 Basin (group D). Station ST/8 marked with \* was sampled in summer season. Kruskal –  
 582 Wallis results for differences between sampling sites are given; significant test results are  
 583 marked with \*\* ( $p < 0.05$ ).

584 Table 8. Spearman's rank correlation analyses among biological and physical parameters. Significant values are marked in bold ( $p < 0.05$ ).

	No of taxa	Density	Biomass	Non-local (r)	Biodiffusion (Db)	Depth	Salinity	Temperature	Gravel	Sand	Mud	BW C <sub>org</sub>	BW N <sub>tot</sub>	BW $\delta^{13}C$	BW $\delta^{15}N$	BW C/N	Sed C <sub>org</sub>	Sed N <sub>tot</sub>	Sed $\delta^{13}C$	Sed $\delta^{15}N$	Sed C/N	SOM	Chl <i>a</i>	Chl <i>a</i> /Phaeo
No of taxa	-	<b>0.9</b>	<b>0.5</b>	<b>0.5</b>	0.0	-0.1	0.2	0.1	0.0	-0.1	<b>0.3</b>	-0.1	0.0	-0.1	-0.2	0.0	-0.2	<b>0.3</b>	<b>0.5</b>	-0.1	<b>-0.6</b>	0.1	<b>0.6</b>	0.2
Density	<b>0.9</b>	-	<b>0.5</b>	<b>0.4</b>	-0.1	-0.2	-0.1	0.0	0.0	-0.1	0.2	-0.1	0.1	-0.1	-0.2	-0.1	-0.2	0.1	0.3	-0.1	<b>-0.3</b>	0.1	<b>0.5</b>	<b>0.3</b>
Biomass	<b>0.5</b>	<b>0.5</b>	-	<b>0.5</b>	<b>0.4</b>	<b>-0.5</b>	-0.2	<b>-0.3</b>	-0.3	<b>-0.4</b>	<b>0.6</b>	<b>0.3</b>	0.0	0.2	<b>0.4</b>	<b>0.4</b>	<b>0.4</b>	<b>0.6</b>	0.2	-0.1	-0.1	<b>0.3</b>	<b>0.4</b>	0.3
Non-local (r)	<b>0.5</b>	<b>0.4</b>	<b>0.5</b>	-	0.3	-0.2	0.1	0.0	-0.1	<b>-0.4</b>	<b>0.5</b>	0.2	0.1	0.1	0.2	0.2	0.2	<b>0.5</b>	<b>0.4</b>	-0.1	<b>-0.3</b>	0.3	<b>0.4</b>	0.1
Biodiffusion (Db)	0.0	-0.1	<b>0.4</b>	0.3	-	<b>-0.6</b>	<b>-0.4</b>	<b>-0.3</b>	<b>-0.3</b>	0.0	0.2	0.2	-0.2	0.0	<b>0.5</b>	<b>0.6</b>	<b>0.6</b>	<b>0.4</b>	-0.2	0.2	<b>0.4</b>	<b>0.3</b>	0.0	0.0

585

### 586 3.4. Storfjorden – seasonal changes

587

588 Bottom water salinity was similar in spring and summer in Storfjorden, respectively  
589 34.5 and 34.1. Bottom water temperature in spring season was  $-0.8\text{ }^{\circ}\text{C}$  and increased to  $4.5\text{ }^{\circ}\text{C}$   
590 (Table 1). Benthic density decreased from  $3625.3\text{ ind./m}^2 \pm 83.9\text{ SE}$  in spring (AX/3) to  
591  $1812.7\text{ ind./m}^2 \pm 229.7\text{ SE}$  in summer (ST/8). Biomass was similar in both seasons ( $172.3$   
592  $\text{g/m}^2 \pm 37.3\text{ SE}$  (spring, AX/3) and  $152.1\text{ g/m}^2 \pm 67.5\text{ SE}$  (summer, ST/8). Non-local transport  
593 rates were similar in spring and summer ( $2.12 \pm 1$  and  $2.09 \pm 0.72\text{ y}^{-1}$  respectively) but  
594 biodiffusion rates increased in summer ( $0.06 \pm 0.04$  in spring and  $0.90 \pm 0.90\text{ cm}^2\text{ y}^{-1}$  in  
595 summer). Significant differences were found for the number of taxa and macrofauna density  
596 between spring and summer seasons (Mann-Whitney U-test;  $Z= 2.3$ ;  $p<0.05$  and  $Z=2.4$ ;  
597  $p<0.05$ , respectively).

598

## 599 4. Discussion

600

601 This is the first complex report on bioturbation activities in spring to summer  
602 transition time conducted over the large area from Svalbard fjords and Barents Sea to deep  
603 basin north off Svalbard. In our study, benthic community variables differentiated four  
604 groups of stations, and this separation was to some extent echoed by the environmental  
605 factors. The benthic community properties further affected the measured benthic activities i.e.  
606 bioturbation rates.

607

### 608 4.1. Benthic community characteristics across the sampled area

609

610 The structure and composition of the benthic communities seemed to be grouped in  
611 four groups of stations, however, the primary variables of the benthic community structure  
612 (e.g., density, biomass) were highly variable within each station. One of the reasons could be  
613 the high variability among replicates that covered only small area of sampled sediment.  
614 Benthic species richness of the region was not well represented in the cores taken for the  
615 experiments at each station due to their small sampling unit (~113 cm<sup>2</sup>). This may have  
616 implications for the results generalization to the sampled areas due to high variability of  
617 benthic density, biomass and consequently on the effects of these on the measured  
618 bioturbation coefficients. However, we assume that we collected the most abundant taxa,  
619 which would likely have the dominant role in mediating bioturbation effect. We have sampled  
620 and identified the benthic organisms in each sediment core where the bioturbation  
621 experiments were processed meaning that we know the organisms responsible of the  
622 measured bioturbation activities.

623 The variability of the quality and quantity of sedimentary OM within each station  
624 impacted benthic community structure. For instance, the lowest quality of SOM (C/N~18)  
625 was found in sandy sediments of Van Mijenfjorden and Hornsund fjords, highlighting  
626 dominance of refractory organic material within the group A. This probably explains the  
627 lowest benthic densities and biomass at these stations. This can be the result of geographical  
628 locations (e.g., water circulation restrictions) and glacial activity in Hornsund, related high  
629 sedimentation rates and high terrestrial OM inputs disturbing benthic fauna (Drewnik et al.,  
630 2016; Włodarska-Kowalczyk and Pearson, 2004). These two stations' communities were  
631 mainly shaped by presence of polychaete *Polycirrus arcticus* and cumacean *Diastylis lucifera*,  
632 and opportunistic cirratulids were among dominants.

633 A high, but variable, B/D ratio was found in Storffjorden (group B), which is the site of  
634 a recurring polynya and has some of the highest productivity in the Barents Sea. The low

635 temperature, presence of a sea ice-edge bloom, very fine grained sediments (muds) indicating  
636 low hydrodynamism, and high  $C_{org}$  and Chl *a* contents in sediments and in bottom waters  
637 promote diverse and high biomass benthic communities with larger individuals burrowing and  
638 feeding deeper (Winkelmann and Knies, 2005). High Chl *a*/Phaeo ratio and large quantities of  
639 Chl *a* within sediments show also a more frequent input of fresh OM because of the presence  
640 of the polynya (Haarpaintner et al., 2001; Vinje, 2001; Winkelman and Knies, 2005). This  
641 community was also diverse, with high dominance of polychaetes (cirratulids, carnivore  
642 *Lumbrineris* sp, and subsurface tube-building conveyor *Maldane sarsi*) and bivalves like  
643 *Yoldia hyperborea* and *Nuculana radiata*. PCO indicated that samples collected in Storfjorden  
644 were correlated with presence of bivalve *Ennucula tenuis* and polychaete *Apistobanchus*  
645 *tulbergi*.

646 The group C, covering stations sampled over the Barents Sea shelf, was highly  
647 variable in terms of community structure and various environmental factors. The southern  
648 Barents Sea station (AX/6) was characterized by similar environmental conditions to the  
649 Storfjorden resulting in the occurrence of fauna with similar characteristics but with a lower  
650 biomass to density ratio. This station was dominated by tube-building conveyor polychaete  
651 *Spiochaetopterus typicus* and *Heteromastus* sp. and bivalve *Macoma* sp. It was characterized  
652 by high amount of SOM but low Chl *a* in the sediments, indicating late bloom/post bloom  
653 conditions, where most of the fresh OM was already utilized by benthic organisms. Lower  
654 Chl *a*/Phaeo ratio also indicates more degraded OM, possibly a result of intensive pelagic  
655 grazing (Morata and Renaud, 2008). This is likely since this station is in the southernmost  
656 location, therefore it was under the strong influence of Atlantic waters and was already in the  
657 late-phase of the phytoplankton bloom (Krause et al., 2018). The other stations from this  
658 group, located in the northern part of Barents Sea e.g. Erik Eriksen Strait, were characterized  
659 by high share of sand but relatively fresh and abundant SOM, though low Chl *a* levels. This is

660 quite similar to stations north of Svalbard (PS/20 and PS/32), although the later was  
661 characterized by higher amounts of Chl *a* present in the sediment related to the bloom in  
662 progress at the time of sampling (Peeken, 2016). This group was characterized by highly  
663 diverse communities (from 36 (AX/6) to 68 (PS/32) number of taxa), however most of them  
664 belonged to either biodiffusors or conveyors.

665 The northern Barents Sea and Nansen Basin (group D) were differentiated from the  
666 other groups by salinity, temperature, depth and occurrence of gravel. The species shaping  
667 communities included polychaetes *Prionospio cirrifera* and *Notoproctus oculatus*. Stations in  
668 group D were seasonally ice covered (including during sampling), and deeper than 400 m.  
669 They were characterized by low amount of Sed C<sub>org</sub> but presence of high OM quality in  
670 bottom water layer, perhaps indicating recent sedimentation. They were characterized by  
671 much lower benthic biomass and higher benthic density which were both decreasing with  
672 increasing depth regardless the bloom stage. Decreasing quality and quantity of OM with  
673 increasing depth, as it was observed in Nansen Basin, are often reflected in spatial variations  
674 in benthic community structure (Carroll et al., 2008) and result in severe energy limitation for  
675 deep-seafloor communities, dominated by small sized-individuals in high densities (Gage and  
676 Tyler, 1991; Bergmann et al., 2009; Grebmeier et al., 1988; Renaud et al., 2008).

677 Long living Arctic benthic fauna reflects carbon export fluxes to the sea bottom but  
678 changes are observed after several years or decades at deep stations (Grebmeier, 2012; Link et  
679 al., 2013). Therefore, it is likely that the bloom stage and current OM delivery to the sea floor  
680 did not directly influence the benthic community structure which is mainly dependent on the  
681 integrated carbon input to the sediments and OM pool available in the sediment. However,  
682 fresh OM arriving to the sea floor can trigger fast benthic response in terms of feeding and  
683 related movement (Morata et al., 2015; Boetius et al., 2013), thus influence the community  
684 functioning.



685

686 *4.2. Bioturbation processes (sediment mixing)*

687

688 Conducting experiments at the large depth gradient posts a challenge of working in  
689 hyperbaric conditions. Although, Glud et al. (1994) showed that in situ measurements of  
690 sediment oxygen demand/oxygen penetration depth were uniformly higher than deck  
691 incubations, the relative differences among stations did not change with depth. Since other  
692 published studies have also not incorporated hyperbaric chambers when estimating sediment  
693 oxygen demand (Boetius et al., 2013), metabolism (Linke et al., 1995), and bioturbation  
694 (Clough et al., 1997), our results, as the relative rates, remain comparable.

695 Both coefficients of bioturbation (non-local transport ( $r$ ) and biodiffusion ( $Db$ ) were  
696 quantified in the stations of groups A, B and C where a higher diversity of bioturbation groups  
697 was recorded among the dominant taxa (Table 4). Stations of the group D, on the contrary,  
698 exhibited lower diversity of functional traits among the dominant taxa with the simultaneous  
699 presence of two groups of sediment mixing (conveyors, biodiffusers) but where only non-  
700 local transport was observed.

701 Species identity and differences in species characteristics, such as feeding mode and  
702 typical burrowing depth, have been previously shown to influence the intensity of  
703 bioturbation (Viitasalo-Frösén et al., 2009; Josefson et al., 2012; Näkki et al., 2017) and  
704 functional diversity can be considered to have more impacts than taxonomic richness (Harvey  
705 et al., 2012; Link et al., 2013). However, interpreting the bioturbation processes and the  
706 assignment of the macrofaunal species to the correct functional group can be challenging.  
707 Short-term experimental studies of sediment mixing provide just essential data for only few  
708 species and results are hard to compare with longer time-scale processes in natural  
709 ecosystems. Also, the same species can have different behavior and belong to another

710 sediment mixing groups across their ranges since species are known to be able to feed in  
711 several different ways and change their feeding and mobility to exploit the food resources  
712 available (Biles et al., 2002). Change in organism feeding behavior will also mean a change in  
713 bioturbation which is reduced as a result of decreasing species diversity and community  
714 biomass, as well as diversity of feeding and bioturbation groups (Mazik and Elliott, 2000). In  
715 general, in our study, the high number of sub-surface deposit feeders, which feed at depth and  
716 transport material to the surface can explain dominance of non-local mixing (Boudreau, 1997;  
717 Gérino et al., 1998). Conveyors were actually omnipresent and the intensity of non-local  
718 transport was variable between stations, and was increasing with increasing species richness,  
719 density and biomass, but also with increasing percentage of mud presence and Chl *a* contents  
720 (Table 8). Since non-local transport is non-continuous, it is usually difficult to link it directly  
721 to benthic biomass (or biovolume) since some movements of particles do not depend only on  
722 animal movements, but also on animal-independent effects (e.g., particles falling down into  
723 the burrows, initial burrows construction). In our study, increasing benthic biomass generated  
724 by high labile OM inputs, seems to have positive effects on the conveying activities and  
725 consequently on the non-local transport rates.

726 In shallow fjords (Van Mijenfjorden and Hornsund, Group A), the benthic  
727 communities were characterized by low bioturbation rates (non-local transport from  $0.21 \pm$   
728  $0.20$  to  $0.60 \pm 0.23 \text{ y}^{-1}$  and biodiffusion from  $0.04 \pm 0.01$  to  $0.07 \pm 0.03 \text{ cm}^{-2} \text{ y}^{-1}$ ). This  
729 similarity between the AX/1 and AX/2 stations of the group A can be explained by the  
730 occurrence of a similar benthic community whose the species have the same functional traits  
731 combination (i.e., feeding, mobility, burrowing depth, burrowing mode and sediment mixing  
732 mode; Table 4) but present in low density and biomass. Biodiffusers (Cirratulidae; Gérino et  
733 al., 1992, 2007), conveyors (*P. arcticus*) and gallery diffusors (*Lumbrineris* sp.; Petch, 1986),

734 both present in those fjords, were probably limited by the lack of fresh OM in the sediments at  
735 the time of sampling.

736 Storfjorden (AX/3, group B), Erik Eriksen Strait (AX/4) and PS/20 (group C) had  
737 similar measured bioturbation rates with high non-local transport and low biodiffusion, and  
738 shared a high biomass contribution of bivalves and maldanid polychaetes. Yoldiids and  
739 maldanids, burrowing deeper into the sediment, are known to be effective conveyors which  
740 can either actively transfer sediment directly into deep layers from the surface, or into surface  
741 layers from deeper layers of the sediments (Bender and Davis, 1984; Smith and Schafer,  
742 1984), respectively. This can explain high non-local transport in these areas.

743 The southern Barents Sea, AX/6, group C, had higher but strongly spatially variable  
744 Db and r by station within the group, with a relatively higher biomass and density of the  
745 organisms (*Spiochaetopterus typicus* (conveyor, Smith and Shafer, 1984) dominating in the  
746 density and *Astarte* sp. (biodiffusor, Queirós et al., 2013) dominating in the biomass. The  
747 reason for that was most likely earlier occurrence of the phytoplankton bloom due to the lack  
748 of sea ice, so at the time of the cruise, late spring/post-bloom conditions and abundant OM  
749 activated rapidly benthic organisms.

750 All deeper and sea ice covered stations in group D, including sea ice covered PS/32  
751 (group C), were dominated by biodiffusers and conveyors (Table 4). Those stations were  
752 characterized by significant non-local transport and unmeasurable biodiffusion. This suggests  
753 that the sediment transport mode by conveyors dominated in the sampled deeper areas  
754 adapted to scarce fresh food availability despite the presence of biodiffusers. This implies a  
755 very low activity by biodiffusers undetectable at the time scale of 10 days of experiment, or  
756 an interfering of such activities with the conveyors species. Typically for communities living  
757 in OM limited environments, these benthic communities were characterized by a low number  
758 of species with low biomass. Giving the low bioturbation rates in the deeper stations, we

759 could actually suppose that time incubation with luminophores superior to 10 days could be  
760 tested in the future experiments in order to insure a more complete transport of tracers  
761 towards deep layers where the benthic community is less active. Since the bioturbation model  
762 takes into account in its calculation this time duration, the final bioturbation coefficient is  
763 however normalized to this time scale, signifying the similar relative comparison between  
764 stations for our experiment remains valid. If we were able to detect measurable biodiffusive  
765 coefficient for the deeper stations for a longer time scale, normalized to the same time unit,  
766 the biodiffusion would be still low because of weak benthic infauna dynamic in such  
767 environments. Our results are, however, similar to the patterns showed by Clough et al.  
768 (1997) who noted low biodiffusive transport ( $0.01$  to  $0.11 \text{ cm}^{-2} \text{ y}^{-1}$ ) by using radioactive tracer  
769 for its deep portions in relationships to the lower benthic biomass due to lower fresh OM  
770 inputs. They found, however, higher surficial sediment biological mixing rates than the  
771 natural sedimentation rates in the Arctic deep sediments, highlighting the importance of  
772 quantifying bioturbation in the Arctic Ocean taking into account its spatial variability. Also,  
773 Soltwedel et al. (2019), using luminophores for experiments that lasted 2 and 4 years, found  
774 low biodiffusion mixing rates at the Long-Term Ecological Research (LTER) observatory  
775 HAUSGARTEN in Fram Strait ( $\sim 0.2 \text{ cm}^{-2} \text{ y}^{-1}$ ). They concluded that the meiofauna, and to a  
776 certain extent megafauna, were the main bioturbators in the deep sea environments. Although,  
777 only macrofauna ( $>500 \mu\text{m}$ ) was identified and was presented as the main responsible of the  
778 bioturbation activities in our study, meiofaunal activities may also explain some of the  
779 patterns that could not be attributed to the changes in the environment or macrofaunal  
780 communities in the deep sea stations. Since the model quantifies bioturbation coefficients of  
781 the entire benthic community, it includes here also the meiofauna activities. Meiofauna is  
782 actually known as the most abundant infauna (Heip et al., 1985; Vanreusel et al., 2010; Rosli  
783 et al., 2016; own data) and as having impact on the bioturbation activities in the first few

784 centimeters of the sediment (Aller and Aller, 1992; Piot et al., 2014; Aschenbroich et al.,  
785 2017; Mäkelä et al., 2018). Therefore, we suggest that also the smaller benthic fractions  
786 should be identified in future studies on Arctic deep infaunal activity in order to find better  
787 infauna variables for explaining the bioturbation measurements.

788

#### 789 4.3. Seasonal changes (Storfjorden station)

790

791 The highest values of non-local transport were reported for Storfjorden and remained  
792 stable during both spring and summer time. The biodiffusion coefficient measured in  
793 Storfjorden during summer was about fifteen times higher compared to measurements  
794 conducted during spring, probably because of the changes in species and functional groups  
795 between the two seasons associated with the more labile OM reaching the seafloor in summer  
796 (Chl *a*/Phaeo~52, Table 3). The dominant taxa in density were Cirratullidae (biodiffusor)  
797 both during spring and summer (31.2 % and 11 %, respectively) and Lumbrineris sp. (gallery  
798 diffusor) (14.1 % and 18.3 %, respectively) while in biomass, *Yoldia hyperborea* (convoyer)  
799 dominated during both seasons (57.4 % and 30.5 %, respectively) (Table 4). Such changes,  
800 i.e. replacement of one large specimen by another large specimen of different species, should  
801 be rather accounted to spatial variability of benthic communities than due to seasonal change  
802 in sampled communities. Also, species such as *Nereis diversicolor* or *M. balthica* are able to  
803 change their feeding mode (suspensive-feeder versus deposit feeder) depending on  
804 environmental conditions (De Goej and Luttikhuisen, 1998; Christensen et al., 2000). It is  
805 also possible that taxa such as Cirratulidae, *Lumbrinereis*, *Yoldia* and *Nuculana* change their  
806 feeding mode with increased OM input from the polynya during the summer just after the  
807 spring bloom, as was observed in other ecosystems or experiments (e.g., Bender and Davis,  
808 1984 for *Yoldia* spp; Rouse and Pleijel, 2001; Kędra et al., 2012 for Cirratulidae).

809 Benthic activities are related to the supply of OM to the seabed (Grassle and Grassle,  
810 1994; Levin and Gooday, 2003; Blake et al., 2009) and biodiffusion intensity can be strongly  
811 dependent on flux of fresh food from overlying waters (Gérino et al., 1998). In shallow  
812 sediments of temperate areas, Duport et al. (2007) found the highest intensity of sediment  
813 mixing (non-local and biodiffusion) during summer in the Thau Lagoon. Also Gérino et al.  
814 (2007) found more rapid non-local transport in spring than in autumn in the Venice Lagoon.  
815 Organic carbon supply generally increases when the PP starts in spring, and peaks with the  
816 bloom and afterwards, over the summer. In the polar areas, Morata et al. (2015) found  
817 minimum biodiffusive activity during the polar night, and high non-local transport after a  
818 pulse of fresh food in experiments conducted in high Arctic fjord in Svalbard. This result  
819 suggests that behavior of benthic species change with the OM input. Also, laboratory  
820 experiments showed that macrofauna can react quickly to food input by increasing their  
821 bioturbation activities (Nogaro et al., 2008). Furthermore, Dauwe et al. (1998) reported  
822 maximum sediment mixing with medium food quality in the study comparing macrofaunal  
823 benthic activity with contrasting food supply in the North Sea. They also showed that the  
824 minimal mixing was observed at the station with high quality OM, and no mixing when low  
825 quality OM was present. This can result from combination of physical and biochemical  
826 factors influencing bioturbation, or changes in species behavior. The other possible  
827 explanation is related to the oxygen conditions in different areas. Both North and Baltic Sea  
828 are areas with high PP and eutrophication. Higher amounts of new OM reaching the sea floor  
829 often result in low oxygen levels leading to anoxic conditions affecting faunal behavior or  
830 even survival (Carstensen et al., 2014). Svalbard fjords and adjacent areas are largely oligo-  
831 and meso- trophic, and well oxygenated regardless the time of the year and intensity of the  
832 spring bloom deposition. We, thus, expect minimal negative impacts of OM deposition on

833 benthic communities. Our results from this limited seasonal comparison suggest that large  
834 inputs of fresh OM to the seabed can trigger bioturbation activities.

835

### 836 **Acknowledgements**

837 This work is a contribution to the Polish National Science Centre (project number  
838 2015/19/B/NZ8/03945 (SeaIceFun) to MK) and the Norwegian Research Council (ARCEX  
839 project #228107). We would like to thank the crew and scientific team for support and  
840 assistance at the sea during the Arctic in Rapid Transition (ART) Network cruise TRANSSIZ  
841 (ARK XXIX/1; PS92) on R/V Polarstern, ARCEX cruise on R/V Helmer Hanssen and SteP  
842 cruise on R/V L'Atalante, especially to Maeve McGovern. We would like to thank Leading  
843 National Research Centre (KNOW) received by the Centre for Polar Studies for the financial  
844 support. Thank you to Aleksandra Winogradow (IOPAN) and Jeremy Devesa (LEMAR) for  
845 their help during CHN analyses. Mobility grants of BO, NM and EM were supported by the  
846 French National Agency under the program "Investissements d'Avenir" (LabexMER: ANR-  
847 10-LABX-19) and by the scientific committee of IUEM to EM. We thank three anonymous  
848 reviewers for their comments, which significantly improved the paper. This paper is a Nereis  
849 Park number 41.

850

### 851 **References:**

- 852 Aller, R.C., Aller, J.Y., 1992. Meiofauna and solute transport in marine muds. *Limnology and*  
853 *Oceanography* 37, 1018–1033. <https://doi.org/10.4319/lo.1992.37.5.1018>
- 854 Anderson, M.J., Gorley, R.N., Clarke, K.R., 2008. PERMANOVA for PRIMER: guide to  
855 software and statistical methods. PRIMER-E Ltd., Plymouth, United Kingdom p. 214.
- 856 Andreassen, I., Wassmann, P., 1998. Vertical flux of phytoplankton and particulate biogenic  
857 matter in the marginal ice zone of the Barents Sea in May 1993. *Marine Ecology*

- 858 Progress Series 170, 1–14. <https://doi.org/10.3354/meps170001>
- 859 Aschenbroich, A., Michaud, E., Gilbert, F., Fromard, F., Alt, A., Le Garrec, V., Bihannic, I.,  
860 De Coninck, A., Thouzeau, G., 2017. Bioturbation functional roles associated with  
861 mangrove development in French Guiana, South America. *Hydrobiologia* 794, 179–  
862 202. <https://doi.org/10.1007/s10750-017-3093-7>
- 863 Bender, K., Davis, W.R., 1984. The effect of feeding by *Yoldia limatula* on bioturbation.  
864 *Ophelia* 23, 91–100. <https://doi.org/10.1080/00785236.1984.10426606>
- 865 Bergmann, M., Dannheim, J., Bauerfeind, E., Klages, M., 2009. Trophic relationships along a  
866 bathymetric gradient at the deep-sea observatory HAUSGARTEN. *Deep Sea Research*  
867 Part I: Oceanographic Research Papers 56, 408–424.  
868 <https://doi.org/10.1016/j.dsr.2008.10.004>
- 869 Berner, R.A., 1980. Early diagenesis. A theoretical approach. Princeton University Press,  
870 Princeton, NJ.
- 871 Biles, C.L., Paterson, D.M., Ford, R.B., Solan, M., Raffaelli, D.G., 2002. Bioturbation,  
872 ecosystem functioning and community structure. *Hydrology and Earth System*  
873 *Sciences* 6, 999–1005. <https://doi.org/10.5194/hess-6-999-2002>
- 874 Blake, J.A., Maciolek, N.J., Ota, A.Y., Williams, I.P., 2009. Long-term benthic infaunal  
875 monitoring at a deep-ocean dredged material disposal site off Northern California.  
876 *Deep Sea Research Part II: Topical Studies in Oceanography* 56, 1775–1803.  
877 <https://doi.org/10.1016/j.dsr2.2009.05.021>
- 878 Błaszczuk, M., Jania, J.A., Kolondra, L., 2013. Fluctuations of tidewater glaciers in Hornsund  
879 Fjord (Southern Svalbard) since the beginning of the 20th century. *Polish Polar*  
880 *Research* 34, 327–352. <https://doi.org/10.2478/popore-2013-0024>
- 881 Blott, S.J., Pye, K., 2001. GRADISTAT: a grain size distribution and statistics package for the  
882 analysis of unconsolidated sediments. *Earth Surface Processes and Landforms* 26,



- 883 1237–1248. <https://doi.org/10.1002/esp.261>
- 884 Boetius, A., Albrecht, S., Bakker, K., Bienhold, C., Felden, J., Fernandez-Mendez, M.,  
885 Hendricks, S., Katlein, C., Lalande, C., Krumpfen, T., Nicolaus, M., Peeken, I., Rabe,  
886 B., Rogacheva, A., Rybakova, E., Somavilla, R., Wenzhofer, F., RV Polarstern ARK27-  
887 3-Shipboard Science Party, 2013. Export of Algal Biomass from the Melting Arctic Sea  
888 Ice. *Science* 339, 1430–1432. <https://doi.org/10.1126/science.1231346>
- 889 Bouchet, V.M.P., Sauriau, P.-G., Debenay, J.-P., Mermillod-Blondin, F., Schmidt, S., Amiard,  
890 J.-C., Dupas, B., 2009. Influence of the mode of macrofauna-mediated bioturbation on  
891 the vertical distribution of living benthic foraminifera: First insight from axial  
892 tomodesitometry. *Journal of Experimental Marine Biology and Ecology* 371, 20–33.  
893 <https://doi.org/10.1016/j.jembe.2008.12.012>
- 894 Boudreau, B.P., 1986. Mathematics of tracer mixing in sediments. 2. Nonlocal mixing and  
895 biological conveyor-belt phenomena. *American Journal of Science* 286, 199-238.
- 896 Boudreau, B.P., 1997. Diagenetic models and their implementation. Springer Verlag, 414 pp.
- 897 Bourgeois, T., Orr, J.C., Resplandy, L., Terhaar, J., Ethé, C., Gehlen, M., Bopp, L., 2016.  
898 Coastal-ocean uptake of anthropogenic carbon. *Biogeosciences* 13, 4167–4185.  
899 <https://doi.org/10.5194/bg-13-4167-2016>
- 900 Carroll, J., Zaborska, A., Papucci, C., Schirone, A., Carroll, M.L., Pempkowiak, J., 2008.  
901 Accumulation of organic carbon in western Barents Sea sediments. *Deep Sea Research*  
902 Part II: Topical Studies in Oceanography 55, 2361–2371.  
903 <https://doi.org/10.1016/j.dsr2.2008.05.005>
- 904 Carstensen, J., Andersen, J.H., Gustafsson, B.G., Conley, D.J., 2014. Deoxygenation of the  
905 Baltic Sea during the last century. *Proceedings of the National Academy of Sciences*  
906 111, 5628–5633. <https://doi.org/10.1073/pnas.1323156111>
- 907 Christensen, B., Vedel, A., Kristensen, E., 2000. Carbon and nitrogen fluxes in sediment

- 908 inhabited by suspension-feeding (*Nereis diversicolor*) and non-suspension-feeding (*N.*  
909 *virens*) polychaetes. *Marine Ecology Progress Series* 192, 203–217.  
910 <https://doi.org/10.3354/meps192203>
- 911 Clarke, K.R., Gorley, R.N., 2006. PRIMER v6: User manual/tutorial. PRIMER-E, Plymouth  
912 UK.
- 913 Clough, L.M., Ambrose, W.G., Kirk Cochran, J., Barnes, C., Renaud, P.E., Aller, R.C., 1997.  
914 Infaunal density, biomass and bioturbation in the sediments of the Arctic Ocean. *Deep*  
915 *Sea Research Part II: Topical Studies in Oceanography* 44, 1683–1704.  
916 [https://doi.org/10.1016/S0967-0645\(97\)00052-0](https://doi.org/10.1016/S0967-0645(97)00052-0)
- 917 Cochrane, S.K.J., Pearson, T.H., Greenacre, M., Costelloe, J., Ellingsen, I.H., Dahle, S.,  
918 Gulliksen, B., 2012. Benthic fauna and functional traits along a Polar Front transect in  
919 the Barents Sea – Advancing tools for ecosystem-scale assessments. *Journal of Marine*  
920 *Systems* 94, 204–217. <https://doi.org/10.1016/j.jmarsys.2011.12.001>
- 921 Codispoti, L.A., Kelly, V., Thessen, A., Matrai, P., Suttles, S., Hill, V., Steele, M., Light, B.,  
922 2013. Synthesis of primary production in the Arctic Ocean: III. Nitrate and phosphate  
923 based estimates of net community production. *Progress in Oceanography* 110, 126–  
924 150. <https://doi.org/10.1016/j.pocean.2012.11.006>
- 925 D’Andrea, A.F., Lopez, G.R., Aller, R.C., 2004. Rapid physical and biological particle mixing  
926 on an intertidal sandflat. *Journal of Marine Research* 62, 67–92.  
927 <https://doi.org/10.1357/00222400460744627>
- 928 Dauwe, B., Herman, P.M.J., Heip, C.H.R., 1998. Community structure and bioturbation  
929 potential of macrofauna at four North Sea stations with contrasting food supply. *Mar*  
930 *Ecol Prog Ser* 173, 67–8317. <https://doi:10.3354/meps173067>
- 931 De Goeij, P., Luttikhuisen, P., 1998. Deep-burying reduces growth in intertidal bivalves: field  
932 and mesocosm experiments with *Macoma balthica*. *Journal of Experimental Marine*

- 933 Biology and Ecology 228, 327–337. [https://doi.org/10.1016/S0022-0981\(98\)00062-8](https://doi.org/10.1016/S0022-0981(98)00062-8)
- 934 Drewnik, A., Węśławski, J.M., Włodarska-Kowalczyk, M., Łącka, M., Promińska, A.,  
935 Zaborska, A., Gluchowska, M., 2016. From the worm's point of view. I: Environmental  
936 settings of benthic ecosystems in Arctic fjord (Hornsund, Spitsbergen). *Polar Biology*  
937 39, 1411–1424. <https://doi.org/10.1007/s00300-015-1867-9>
- 938 Duchêne, J., Rosenberg, R., 2001. Marine benthic faunal activity patterns on a sediment  
939 surface assessed by video numerical tracking. *Marine Ecology Progress Series* 223,  
940 113–119. <https://doi.org/10.3354/meps223113>
- 941 Duport, E., Gilbert, F., Poggiale, J.-C., Dedieu, K., Rabouille, C., Stora, G., 2007. Benthic  
942 macrofauna and sediment reworking quantification in contrasted environments in the  
943 Thau Lagoon. *Estuarine, Coastal and Shelf Science* 72, 522–533.  
944 <https://doi.org/10.1016/j.ecss.2006.11.018>
- 945 Fauchald, K., Jumars, P.A., 1979. The diet of worms: a study of polychaete feeding guilds.  
946 *Oceanogr Mar Biol Annu Rev* 17, 193–284.
- 947 Fernández-Méndez, M., Katlein, C., Rabe, B., Nicolaus, M., Peeken, I., Bakker, K., Flores,  
948 H., Boetius, A., 2015. Photosynthetic production in the central Arctic Ocean during the  
949 record sea-ice minimum in 2012. *Biogeosciences* 12, 3525–3549.  
950 <https://doi.org/10.5194/bg-12-3525-2015>
- 951 Fetzer, I., Lønne, O.J., Pearson, T., 2002. The distribution of juvenile benthic invertebrates  
952 in an Arctic glacial fjord. *Polar Biol* 25, 303–315.
- 953 Fisher, J.B., Lick, W.J., McCall, P.L., Robbins, J.A., 1980. Vertical mixing of lake sediments  
954 by tubificid oligochaetes. *Journal of Geophysical Research* 85 (C7), 3997–4006.  
955 <https://doi.org/10.1029/JC085iC07p03997>
- 956 François, F., Delegré, K., Gilbert, F., Stora G., 1999. Specific variability within functional  
957 groups. Study of the sediment reworking of two Veneridae bivalves, *Ruditapes*

- 958 decussatus and *Venerupis aurea*. *C. R. Acad. Sci. Paris*, 322, 339-345.
- 959 François, F., Gérino, M., Stora, G., Durbec, J., Poggiale, J., 2002. Functional approach to  
960 sediment reworking by gallery-forming macrobenthic organisms: modeling and  
961 application with the polychaete *Nereis diversicolor*. *Marine Ecology Progress Series*  
962 229, 127–136. <https://doi.org/10.3354/meps229127>
- 963 François, F., Poggiale, J.-C., Durbec, J.-P., Stora, G., 2001. A new model of bioturbation for a  
964 functional approach to sediment reworking resulting from macrobenthic communi-  
965 ties. In: Aller JY, Woodin SA, Aller RC (eds) *Organism–sediment interactions*.  
966 University of South Carolina Press, Columbia, p 73–86.
- 967 François, F., Poggiale, J.-C., Durbec, J.-P., Stora, G., 1997. A new approach for the modelling  
968 of sediment reworking induced by a macrobenthic community. *Acta Biotheor.* 45, 295–  
969 319.
- 970 Gage, J., Tyler, P., 1991. *Deep-Sea Biology: A Natural History of Organisms at the Deep-Sea*  
971 *Floor*. Cambridge University Press, New York.
- 972 Gardner, L.R., Sharma, P., Moore, W.S., 1987. A regeneration model for the effect of  
973 bioturbation by fiddler crabs on <sup>210</sup>Pb profiles in salt marsh sediments. *Journal of*  
974 *Environmental Radioactivity* 5, 25–36.
- 975 Gérino, M., 1992. *Étude expérimentale de la bioturbation en milieu littoral et profond*.  
976 *Doctoral dissertation, Université Aix-Marseille II*. 196 pp.
- 977 Gérino, M., Aller, R.C., Lee, C., Cochran, J.K., Aller, J.Y., Green, M.A., Hirschberg, D., 1998.  
978 *Comparison of Different Tracers and Methods Used to Quantify Bioturbation During a*  
979 *Spring Bloom: <sup>234</sup>Thorium, Luminophores and Chlorophylla*. *Estuarine, Coastal and*  
980 *Shelf Science* 46, 531–547. <https://doi.org/10.1006/ecss.1997.0298>
- 981 Gérino, M., Frignani, M., Mugnai, C., Bellucci, L.G., Prevedelli, D., Valentini, A., Castelli,  
982 A., Delmotte, S., Sauvage, S., 2007. Bioturbation in the Venice Lagoon: Rates and

- 983 relationship to organisms. *Acta Oecologica* 32, 14–25.  
984 <https://doi.org/10.1016/j.actao.2007.02.003>
- 985 Gilbert, F., Hulth, S., Grossi, V., Poggiale, J.-C., Desrosiers, G., Rosenberg, R., Gérino, M.,  
986 François-Carcaillet, F., Michaud, E., Stora, G., 2007. Sediment reworking by marine  
987 benthic species from the Gullmar Fjord (Western Sweden): Importance of faunal  
988 biovolume. *Journal of Experimental Marine Biology and Ecology* 348, 133–144.  
989 <https://doi.org/10.1016/j.jembe.2007.04.015>
- 990 Gingras, M.K., Pemberton, S.G., Dashtgard, S., Dafoe, L., 2008. How fast do marine  
991 invertebrates burrow? *Palaeogeography, Palaeoclimatology, Palaeoecology* 270, 280–  
992 286. <https://doi.org/10.1016/j.palaeo.2008.07.015>
- 993 Glud, R.N., Gundersen, J.K., Barker Jørgensen, B., Revsbech, N.P., Schulz, H.D., 1994.  
994 Diffusive and total oxygen uptake of deep-sea sediments in the eastern South Atlantic  
995 Ocean: in situ and laboratory measurements. *Deep Sea Research Part I: Oceanographic*  
996 *Research Papers* 41, 1767–1788. [https://doi.org/10.1016/0967-0637\(94\)90072-8](https://doi.org/10.1016/0967-0637(94)90072-8)
- 997 Gogina, M., Morys, C., Forster, S., Gräwe, U., Friedland, R., Zettler, M.L., 2017. Towards  
998 benthic ecosystem functioning maps: Quantifying bioturbation potential in the German  
999 part of the Baltic Sea. *Ecological Indicators* 73, 574–588.  
1000 <https://doi.org/10.1016/j.ecolind.2016.10.025>
- 1001 Gosselin, M., Levasseur, M., Wheeler, P.A., Horner, R.A., Booth, B.C., 1997. New  
1002 measurements of phytoplankton and ice algal production in the Arctic Ocean. *Deep Sea*  
1003 *Research Part II: Topical Studies in Oceanography* 44, 1623–1644.  
1004 [https://doi.org/10.1016/S0967-0645\(97\)00054-4](https://doi.org/10.1016/S0967-0645(97)00054-4)
- 1005 Grassle, J.F., Grassle, J.P., 1994. Notes from the abyss: the effects of a patchy supply of  
1006 organic material and larvae on soft-sediment benthic communities. In: Giller, P.S.,  
1007 Hildrew, A.G., Raffaelli, D.G. (Eds.), *Aquatic Ecology: Scale, Pattern and Process*.

- 1008 Blackwell, Oxford, pp. 499–515.
- 1009 Grebmeier, J.M., 2012. Shifting Patterns of Life in the Pacific Arctic and Sub-Arctic Seas.  
1010 Annual Review of Marine Science 4, 63–78. [https://doi.org/10.1146/annurev-marine-](https://doi.org/10.1146/annurev-marine-120710-100926)  
1011 [120710-100926](https://doi.org/10.1146/annurev-marine-120710-100926)
- 1012 Grebmeier, J.M., Cooper, L.W., Feder, H.M., Sirenko, B.I., 2006. Ecosystem dynamics of the  
1013 Pacific-influenced Northern Bering and Chukchi Seas in the Amerasian Arctic.  
1014 Progress in Oceanography 71, 331–361. <https://doi.org/10.1016/j.pocean.2006.10.001>
- 1015 Grebmeier, J.M, McRoy, C., Feder, H., 1988. Pelagic-benthic coupling on the shelf of the  
1016 northern Bering and Chukchi Seas. I. Food supply source and benthic bio-mass. Marine  
1017 Ecology Progress Series 48, 57–67. <https://doi.org/10.3354/meps048057>
- 1018 Haarpaintner, J., Haugan, P.M., Gascard, J.-C., 2001. Interannual variability of the Storfjorden  
1019 (Svalbard) ice cover and ice production observed by ERS-2 SAR. Annals of Glaciology  
1020 33, 430–436. <https://doi.org/10.3189/172756401781818392>
- 1021 Harvey, E., Séguin, A., Nozais, C., Archambault, P., Gravel, D., 2013. Identity effects  
1022 dominate the impacts of multiple species extinctions on the functioning of complex  
1023 food webs. Ecology 94, 169–179. <https://doi.org/10.1890/12-0414.1>
- 1024 Heip C, Vincx M, Vranken G. 1985. The ecology of marine nematodes. Oceanography and  
1025 Marine Biology: An Annual Review 23, 399–489.
- 1026 Holm-Hansen, O., Lorenzen, C.J., Holms, R.W., Strickland, J.D., 1965. Fluorometric  
1027 determination of chlorophyll. J Conseil Int pour l'Exploration de la Mer 30, 3–15.
- 1028 Jørgensen, L.L., Ljubin, P., Skjoldal, H.R., Ingvaldsen, R.B., Anisimova, N., Manushin, I.,  
1029 2015. Distribution of benthic megafauna in the Barents Sea: baseline for an ecosystem  
1030 approach to management. ICES Journal of Marine Science 72, 595–613.  
1031 <https://doi.org/10.1093/icesjms/fsu106>
- 1032 Josefson, A., Norkko, J., Norkko, A., 2012. Burial and decomposition of plant pigments in

- 1033 surface sediments of the Baltic Sea: role of oxygen and benthic fauna. *Marine Ecology*  
1034 *Progress Series* 455, 33–49. <https://doi.org/10.3354/meps09661>
- 1035 Kędra, M., Kuliński, K., Walkusz, W., Legeżyńska, J., 2012. The shallow benthic food web  
1036 structure in the high Arctic does not follow seasonal changes in the surrounding  
1037 environment. *Estuarine, Coastal and Shelf Science* 114, 183–191.  
1038 <https://doi.org/10.1016/j.ecss.2012.08.015>
- 1039 Kędra, M., Pabis, K., Gromisz, S., Węśławski, J.M., 2013. Distribution patterns of polychaete  
1040 fauna in an Arctic fjord (Hornsund, Spitsbergen). *Polar Biology* 36, 1463–1472.  
1041 <https://doi.org/10.1007/s00300-013-1366-9>
- 1042 Kennedy, P., Kennedy, H., Papadimitriou, S., 2005. The effect of acidification on the  
1043 determination of organic carbon, total nitrogen and their stable isotopic composition in  
1044 algae and marine sediment. *Rapid Communications in Mass Spectrometry* 19, 1063–  
1045 1068. <https://doi.org/10.1002/rcm.1889>
- 1046 Knaust, D., Bromley, R.G., 2012. Trace fossils as indicators of sedimentary environments.  
1047 *Developments in sedimentology*, vol 64. Elsevier, Amsterdam.
- 1048 Konovalov, D., Renaud, P.E., Berge, J., Voronkov, A.Y., Cochrane, S.K.J., 2010.  
1049 Contaminants, benthic communities, and bioturbation: potential for PAH mobilisation  
1050 in Arctic sediments. *Chemistry and Ecology* 26, 197–208.  
1051 <https://doi.org/10.1080/02757541003789058>
- 1052 Krause, J.W., Duarte, C.M., Marquez, I.A., Assmy, P., Fernández-Méndez, M., Wiedmann, I.,  
1053 Wassmann, P., Kristiansen, S., Agustí, S., 2018. Biogenic silica production and diatom  
1054 dynamics in the Svalbard region during spring. *Biogeosciences Discussions* 1–25.  
1055 <https://doi.org/10.5194/bg-2018-226>
- 1056 Kristensen, E., Penha-Lopes, G., Delefosse, M., Valdemarsen, T., Quintana, C., Banta, G.,  
1057 2012. What is bioturbation? The need for a precise definition for fauna in aquatic

- 1058 sciences. Marine Ecology Progress Series 446, 285–302.  
1059 <https://doi.org/10.3354/meps09506>
- 1060 Kure, L.K., Forbes, T.L., 1997. Impact of bioturbation by *Arenicola marina* on the fate of  
1061 particle-bound fluoranthene. Marine Ecology Progress Series 156, 157–166.
- 1062 Leu, E., Wiktor, J., Søreide, J., Berge, J., Falk-Petersen, S., 2010. Increased irradiance reduces  
1063 food quality of sea ice algae. Marine Ecology Progress Series 411, 49–60.  
1064 <https://doi.org/10.3354/meps08647>
- 1065 Levin, L.A., Gooday, A.J., 2003. The Deep Atlantic Ocean Chapter 5. In: Tyler, P.A. (Ed.),  
1066 Ecosystems of the Deep Oceans. Ecosystems of the World 28. Elsevier, Amsterdam,  
1067 pp. 111–178.
- 1068 Link, H., Piepenburg, D., Archambault, P., 2013. Are Hotspots Always Hotspots? The  
1069 Relationship between Diversity, Resource and Ecosystem Functions in the Arctic.  
1070 PLoS ONE 8, e74077. <https://doi.org/10.1371/journal.pone.0074077>
- 1071 Linke, P., Altenbach, A.V., Graf, G., Heeger, T., 1995. Response of deep-sea benthic  
1072 foraminifera to a simulated sedimentation event. Journal of Foraminiferal Research 25,  
1073 75-82. <https://doi.org/10.2113/gsjfr.25.1.75>
- 1074 Maire, O., Duchêne, J.C., Grémare, A., Malyuga, V.S., Meysman, F.J.R., 2007. A comparison  
1075 of sediment reworking rates by the surface deposit-feeding bivalve *Abra ovata* during  
1076 summertime and wintertime, with a comparison between two models of sediment  
1077 reworking. Journal of Experimental Marine Biology and Ecology 343, 21–36.  
1078 <https://doi.org/10.1016/j.jembe.2006.10.052>
- 1079 Maiti, K., Carroll, J., Benitez-Nelson, C.R., 2010. Sedimentation and particle dynamics in the  
1080 seasonal ice zone of the Barents Sea. Journal of Marine Systems 79, 185–198.  
1081 <https://doi.org/10.1016/j.jmarsys.2009.09.001>
- 1082 Mäkelä, A., Witte, U., Archambault, P., 2018. Short-term processing of ice algal- and



- 1083 phytoplankton-derived carbon by Arctic benthic communities revealed through isotope  
1084 labelling experiments. *Marine Ecology Progress Series* 600, 21–39.  
1085 <https://doi.org/10.3354/meps12663>
- 1086 Mazik, K., Elliott, M., 2000. The effects of chemical pollution on the bioturbation potential of  
1087 estuarine intertidal mudflats. *Helgoland Marine Research* 54, 99–109.  
1088 <https://doi.org/10.1007/s101520050008>
- 1089 McClintic, M.A., DeMaster, D.J., Thomas, C.J., Smith, C.R., 2008. Testing the  
1090 FOODBANCS hypothesis: Seasonal variations in near-bottom particle flux,  
1091 bioturbation intensity, and deposit feeding based on  $^{234}\text{Th}$  measurements. *Deep Sea*  
1092 *Research Part II: Topical Studies in Oceanography* 55, 2425–2437.  
1093 <https://doi.org/10.1016/j.dsr2.2008.06.003>
- 1094 McMeans, B.C., McCann, K.S., Humphries, M., Rooney, N., Fisk, A.T., 2015. Food Web  
1095 Structure in Temporally-Forced Ecosystems. *Trends in Ecology & Evolution* 30, 662–  
1096 672. <https://doi.org/10.1016/j.tree.2015.09.001>
- 1097 McMinn, A., Pankowskii, A., Ashworth, C., Bhagooli, R., Ralph, P., Ryan, K., 2010. In situ  
1098 net primary productivity and photosynthesis of Antarctic sea ice algal, phytoplankton  
1099 and benthic algal communities. *Marine Biology* 157, 1345–1356.  
1100 <https://doi.org/10.1007/s00227-010-1414-8>
- 1101 Mermillod-Blondin, F., Marie, S., Desrosiers, G., Long, B., de Montety, L., Michaud, E.,  
1102 Stora, G., 2003. Assessment of the spatial variability of intertidal benthic communities  
1103 by axial tomodesitometry: importance of fine-scale heterogeneity. *Journal of*  
1104 *Experimental Marine Biology and Ecology* 287, 193–208.  
1105 [https://doi.org/10.1016/S0022-0981\(02\)00548-8](https://doi.org/10.1016/S0022-0981(02)00548-8)
- 1106 Meysman, F.J.R., Boudreau, B.P., Middelburg, J.J., 2003. New developments in the modelling  
1107 of bioturbation in aquatic sediments: relations between local, non-local, discrete and

- 1108 continuous models. *Terramare* 12, 91-93.
- 1109 Michaud E., 2006. Effet of the Functional ecology of *Macoma balthica* community (St  
1110 Lawrence estuary, Quebec, Canada) on biogeochemical fluxes at the sediment-water  
1111 interface and on sediment mixing. PhD Thesis. University of du Québec à Rimouski et  
1112 Université de la Méditerranée, Aix-Marseille II, 237p.
- 1113 Michaud, E., Desrosiers, G., Mermillod-Blondin, F., Sundby, B., Stora, G., 2005. The  
1114 functional group approach to bioturbation: The effects of biodiffusers and gallery-  
1115 diffusers of the *Macoma balthica* community on sediment oxygen uptake. *Journal of*  
1116 *Experimental Marine Biology and Ecology* 326, 77–88.  
1117 <https://doi.org/10.1016/j.jembe.2005.05.016>
- 1118 Michaud, E., Desrosiers, G., Mermillod-Blondin, F., Sundby, B., Stora, G., 2006. The  
1119 functional group approach to bioturbation: II. The effects of the *Macoma balthica*  
1120 community on fluxes of nutrients and dissolved organic carbon across the sediment–  
1121 water interface. *Journal of Experimental Marine Biology and Ecology* 337, 178–189.  
1122 <https://doi.org/10.1016/j.jembe.2006.06.025>
- 1123 Montserrat, F., Van Colen, C., Provoost, P., Milla, M., Ponti, M., Van den Meersche, K.,  
1124 Ysebaert, T., Herman, P.M.J., 2009. Sediment segregation by biodiffusing bivalves.  
1125 *Estuarine, Coastal and Shelf Science* 83, 379–391.  
1126 <https://doi.org/10.1016/j.ecss.2009.04.010>
- 1127 Morata, N., Michaud, E., Włodarska-Kowalczyk, M., 2015. Impact of early food input on the  
1128 Arctic benthos activities during the polar night. *Polar Biology* 38, 99–114.  
1129 <https://doi.org/10.1007/s00300-013-1414-5>
- 1130 Morata, N., Renaud, P.E., 2008. Sedimentary pigments in the western Barents Sea: A  
1131 reflection of pelagic–benthic coupling? *Deep Sea Research Part II: Topical Studies in*  
1132 *Oceanography* 55, 2381–2389. <https://doi.org/10.1016/j.dsr2.2008.05.004>

- 1133 Mulsow, S., Landrum, P., Robbins, J., 2002. Biological mixing responses to sublethal  
1134 concentrations of DDT in sediments by *Heteromastus filiformis* using a <sup>137</sup>Cs marker  
1135 layer technique. *Marine Ecology Progress Series* 239, 181–191.  
1136 <https://doi.org/10.3354/meps239181>
- 1137 Näkki, P., Setälä, O., Lehtiniemi, M., 2017. Bioturbation transports secondary microplastics to  
1138 deeper layers in soft marine sediments of the northern Baltic Sea. *Marine Pollution*  
1139 *Bulletin* 119, 255–261. <https://doi.org/10.1016/j.marpolbul.2017.03.065>
- 1140 Needham, H.R., Pilditch, C.A., Lohrer, A.M., Thrush, S.F., 2011. Context-Specific  
1141 Bioturbation Mediates Changes to Ecosystem Functioning. *Ecosystems* 14, 1096–1109.  
1142 <https://doi.org/10.1007/s10021-011-9468-0>
- 1143 Nogaro, G., Charles, F., de Mendonça, J.B., Mermillod-Blondin, F., Stora, G., François-  
1144 Carcaillet, F., 2008. Food supply impacts sediment reworking by *Nereis diversicolor*.  
1145 *Hydrobiologia* 598, 403–408. <https://doi.org/10.1007/s10750-007-9135-9>
- 1146 Olli, K., Wexels Riser, C., Wassmann, P., Ratkova, T., Arashkevich, E., Pasternak, A., 2002.  
1147 Seasonal variation in vertical flux of biogenic matter in the marginal ice zone and the  
1148 central Barents Sea. *Journal of Marine Systems* 38, 189–204.  
1149 [https://doi.org/10.1016/S0924-7963\(02\)00177-X](https://doi.org/10.1016/S0924-7963(02)00177-X)
- 1150 Ouellette, D., Desrosiers, G., Gagne, J., Gilbert, F., Poggiale, J., Blier, P., Stora, G., 2004.  
1151 Effects of temperature on in vitro sediment reworking processes by a gallery  
1152 biodiffusor, the polychaete *Neanthes virens*. *Marine Ecology Progress Series* 266, 185–  
1153 193. <https://doi.org/10.3354/meps266185>
- 1154 Ozhigin, V. K., Ingvaldsen, R. B., Loeng, H., Boitsov, V., Karsakov, A., 2011. Introduction to  
1155 the Barents Sea. In *The Barents Sea. Ecosystem, resources, management. Half a*  
1156 *century of Russian-Norwegian cooperation*, pp. 315–328. Ed. by T. Jakobsen, and V. K.  
1157 Ozhigin. Tapir Academic Press, Trondheim.

- 1158 Pathirana, I., Knies, J., Felix, M., Mann, U., 2013. Towards an improved organic carbon  
1159 budget for the Barents Sea shelf, marginal Arctic Ocean. *Climate of the Past*  
1160 *Discussions* 9, 4939–4986. <https://doi.org/10.5194/cpd-9-4939-2013>
- 1161 Peeken, I., 2016. The Expedition PS92 of the Research Vessel POLARSTERN to the Arctic  
1162 Ocean in 2015, *Berichte zur Polar und Meeresforschung* =Reports on polar and marine  
1163 research, Bremerhaven, Alfred Wegener Institute for Polar and Marine Research 694 ,  
1164 153 p. [https://doi.org/10.2312/BzPM\\_0694\\_2016](https://doi.org/10.2312/BzPM_0694_2016)
- 1165 Petch, D.A., 1986. Selective deposit-feeding by *Lumbrineris* cf. *latreilli* (Polychaeta:  
1166 *Lumbrineridae*), with a new method for assessing selectivity by deposit-feeding  
1167 organisms. *Marine Biology* 93, 443-448.
- 1168 Piot, A., Nozais, C., Archambault, P., 2014. Meiofauna affect the macrobenthic biodiversity-  
1169 ecosystem functioning relationship. *Oikos* 123, 203–213.  
1170 <https://doi.org/10.1111/j.1600-0706.2013.00631.x>
- 1171 Queirós, A.M., Birchenough, S.N.R., Bremner, J., Godbold, J.A., Parker, R.E., Romero-  
1172 Ramirez, A., Reiss, H., Solan, M., Somerfield, P.J., Van Colen, C., Van Hoey, G.,  
1173 Widdicombe, S., 2013. A bioturbation classification of European marine infaunal  
1174 invertebrates. *Ecology and Evolution* 3, 3958–3985. <https://doi.org/10.1002/ece3.769>
- 1175 Quintana, C.O., Tang, M., Kristensen, E., 2007. Simultaneous study of particle reworking,  
1176 irrigation transport and reaction rates in sediment bioturbated by the polychaetes  
1177 *Heteromastus* and *Marenzelleria*. *Journal of Experimental Marine Biology and Ecology*  
1178 352, 392–406. <https://doi.org/10.1016/j.jembe.2007.08.015>
- 1179 Rasmussen, T.L., Thomsen, E., 2014. Brine formation in relation to climate changes and ice  
1180 retreat during the last 15,000 years in Storfjorden, Svalbard, 76-78°N.  
1181 *Paleoceanography* 29, 911–929. <https://doi.org/10.1002/2014PA002643>
- 1182 Renaud, P.E., Morata, N., Carroll, M.L., Denisenko, S.G., Reigstad, M., 2008. Pelagic–

- 1183 benthic coupling in the western Barents Sea: Processes and time scales. *Deep Sea*  
1184 *Research Part II: Topical Studies in Oceanography* 55, 2372–2380.  
1185 <https://doi.org/10.1016/j.dsr2.2008.05.017>
- 1186 Rosli, N., Leduc, D., Rowden, A.A., Clark, M.R., Probert, P.K., Berkenbusch, K., Neira, C.,  
1187 2016. Differences in meiofauna communities with sediment depth are greater than  
1188 habitat effects on the New Zealand continental margin: implications for vulnerability to  
1189 anthropogenic disturbance. *PeerJ* 4, e2154. <https://doi.org/10.7717/peerj.2154>
- 1190 Rouse, G.W., Pleijel, F., 2001. *Polychaetes*. Oxford University Press, New York, 354 pp.
- 1191 Sakshaug, E., 2004. Primary and Secondary Production in the Arctic Seas. In: Stein R.,  
1192 MacDonald R.W. (eds) *The Organic Carbon Cycle in the Arctic Ocean*. Springer,  
1193 Berlin, Heidelberg.
- 1194 Sandnes, J., Forbes, T., Hansen, R., Sandnes, B., 2000. Influence of particle type and faunal  
1195 activity on mixing of di(2-ethylhexyl)phthalate (DEHP) in natural sediments. *Marine*  
1196 *Ecology Progress Series*. 197, 151–167.
- 1197 Shick, J.M., 1976. Physiological and behavioral responses to hypoxia and hydrogen sulfide in  
1198 the infaunal asteroid *Ctenodiscus crispatus*. *Marine Biology* 37, 279–289.  
1199 <https://doi.org/10.1007/BF00387613>
- 1200 Shields, M.A., Kedra, M., 2009. A deep burrowing sipunculan of ecological and geochemical  
1201 importance. *Deep Sea Research Part I: Oceanographic Research Papers* 56, 2057–2064.  
1202 <https://doi.org/10.1016/j.dsr.2009.07.006>
- 1203 Skarðhamar, J., Svendsen, H., 2010. Short-term hydrographic variability in a stratified Arctic  
1204 fjord. *Geological Society, London, Special Publications* 344, 51–60.  
1205 <https://doi.org/10.1144/SP344.5>
- 1206 Skogseth, R., Fer, I., Haugan, P.M., 2005. Dense-water production and overflow from an  
1207 arctic coastal polynya in Storfjorden, in: Drange, H., Dokken, T., Furevik, T., Gerdes,

- 1208 R., Berger, W. (Eds.), Geophysical Monograph Series. American Geophysical Union,  
1209 Washington, D. C., pp. 73–88. <https://doi.org/10.1029/158GM07>
- 1210 Smith, J.N., Schafer, C.T., 1984. Bioturbation processes in continental slope and rise  
1211 sediments delineated by Pb-210, microfossil and textural indicators. Journal of Marine  
1212 Research 42, 1117–1145. <https://doi.org/10.1357/002224084788520738>
- 1213 Smoła, Z.T., Tatarek, A., Wiktor, J.M., Wiktor, J.M.W., Kubiszyn, A., Węśławski, J.M., 2017.  
1214 Primary producers and production in Hornsund and Kongsfjorden – comparison of two  
1215 fjord systems. Polish Polar Research 38, 351–373. [https://doi.org/10.1515/popore-](https://doi.org/10.1515/popore-2017-0013)  
1216 [2017-0013](https://doi.org/10.1515/popore-2017-0013)
- 1217 Soltwedel, T., Hasemann, C., Vedenin, A., Bergmann, M., Taylor, J., Krauß, F., 2019.  
1218 Bioturbation rates in the deep Fram Strait: Results from in situ experiments at the arctic  
1219 LTER observatory HAUSGARTEN. Journal of Experimental Marine Biology and  
1220 Ecology 511, 1–9. <https://doi.org/10.1016/j.jembe.2018.11.001>
- 1221 Søreide, J.E., Falk-Petersen, S., Hegseth, E.N., Hop, H., Carroll, M.L., Hobson, K.A.,  
1222 Blachowiak-Samolyk, K., 2008. Seasonal feeding strategies of Calanus in the high-  
1223 Arctic Svalbard region. Deep Sea Research Part II: Topical Studies in Oceanography  
1224 55, 2225–2244. <https://doi.org/10.1016/j.dsr2.2008.05.024>
- 1225 Søreide, J.E., Hop, H., Falk-Petersen, S., Hegseth, E.N., Carroll, M.L., 2006. Seasonal food  
1226 web structures and sympagic-pelagic coupling in the European Arctic revealed by  
1227 stable isotopes and a two-source food web model. Progress in Oceanography 71, 59–  
1228 87. <https://doi.org/10.1016/j.pocean.2006.06.001>
- 1229 Stead, R.A., Thompson, R.J., 2006. The influence of an intermittent food supply on the  
1230 feeding behaviour of *Yoldia hyperborea* (Bivalvia: Nuculanidae). Journal of  
1231 Experimental Marine Biology and Ecology 332, 37–48.  
1232 <https://doi.org/10.1016/j.jembe.2005.11.001>

- 1233 Svendsen, H., Beszczynska-Møller, A., Hagen, J.O., Lefauconnier, B., Tverberg, V., Gerland,  
1234 S., Ørb, J.B., Zajaczkowski, M., Azzolini, R., Bruland, O., Wiencke, C., Winther, J.-G.,  
1235 Dallmann, W., 2002. The physical environment of Kongsfjorden–Krossfjorden, an  
1236 Arctic fjord system in Svalbard. *Polar Research* 21, 133-166.
- 1237 Tamelander, T., Reigstad, M., Hop, H., Carroll, M.L., Wassmann, P., 2008. Pelagic and  
1238 sympagic contribution of organic matter to zooplankton and vertical export in the  
1239 Barents Sea marginal ice zone. *Deep Sea Research Part II: Topical Studies in*  
1240 *Oceanography* 55, 2330–2339. <https://doi.org/10.1016/j.dsr2.2008.05.019>
- 1241 Tamelander, T., Renaud, P.E., Hop, H., Carroll, M.L., Ambrose Jr., W.G., Hobson, K.A., 2006.  
1242 Trophic relationships and pelagic–benthic coupling during summer in the Barents Sea  
1243 Marginal Ice Zone revealed by stable carbon and nitrogen isotope measurements.  
1244 *Marine Ecology Progress Series* 310, 33–46.
- 1245 Teal, L., Bulling, M., Parker, E., Solan, M., 2008. Global patterns of bioturbation intensity  
1246 and mixed depth of marine soft sediments. *Aquatic Biology* 2, 207–218.  
1247 <https://doi.org/10.3354/ab00052>
- 1248 Van Leeuwe, M.A., Tedesco, L., Arrigo, K.R., Assmy, P., Campbell, K., Meiners, K.M.,  
1249 Rintala, J.-M., Selz, V., Thomas, D.N., Stefels, J., Deming, J.W., 2018. Microalgal  
1250 community structure and primary production in Arctic and Antarctic sea ice: A  
1251 synthesis. *Elem Sci Anth* 6. <https://doi.org/10.1525/elementa.267>
- 1252 Vanreusel, A., Fonseca, G., Danovaro, R., Da Silva, M.C., Esteves, A.M., Ferrero, T., Gad, G.,  
1253 Galtsova, V., Gambi, C., Da Fonsêca Genevois, V., Ingels, J., Ingole, B., Lampadariou,  
1254 N., Merckx, B., Miljutin, D., Miljutina, M., Muthumbi, A., Netto, S., Portnova, D.,  
1255 Radziejewska, T., Raes, M., Tchesunov, A., Vanaverbeke, J., Van Gaever, S., Venekey,  
1256 V., Bezerra, T.N., Flint, H., Copley, J., Pape, E., Zeppilli, D., Martinez, P.A., Galeron,  
1257 J., 2010. The contribution of deep-sea macrohabitat heterogeneity to global nematode

- 1258 diversity: Nematode diversity and habitat heterogeneity. *Marine Ecology* 31, 6–20.  
1259 <https://doi.org/10.1111/j.1439-0485.2009.00352.x>
- 1260 Venturini, N., Pires-Vanin, A.M.S., Salhi, M., Bessonart, M., Muniz, P., 2011. Polychaete  
1261 response to fresh food supply at organically enriched coastal sites: Repercussion on  
1262 bioturbation potential and trophic structure. *Journal of Marine Systems* 88, 526–541.  
1263 <https://doi.org/10.1016/j.jmarsys.2011.07.002>
- 1264 Viitasalo-Frösén, S., Laine, A., Lehtiniemi, M., 2009. Habitat modification mediated by  
1265 motile surface stirrers versus semi-motile burrowers: potential for a positive feedback  
1266 mechanism in a eutrophied ecosystem. *Marine Ecology Progress Series* 376, 21–32.  
1267 <https://doi.org/10.3354/meps07788>
- 1268 Vinje, T., 2001. Anomalies and Trends of Sea-Ice Extent and Atmospheric Circulation in the  
1269 Nordic Seas during the Period 1864–1998. *Journal of Climate* 14, 255–267.  
1270 [https://doi.org/10.1175/1520-0442\(2001\)014<0255:AATOSI>2.0.CO;2](https://doi.org/10.1175/1520-0442(2001)014<0255:AATOSI>2.0.CO;2)
- 1271 Vinje, T., 2009. Sea-ice. In *Ecosystem Barents Sea*, pp. 65–82. Ed. by E. Sakshaug, K.  
1272 Kovacs, and G. Johnsen. Tapir Academic Press, Trondheim, Norway. 62-82 p.
- 1273 Winkelmann, D., Knies, J., 2005. Recent distribution and accumulation of organic carbon on  
1274 the continental margin west off Spitsbergen. *Geochemistry, Geophysics, Geosystems* 6,  
1275 1-22. <https://doi.org/10.1029/2005GC000916>
- 1276 Włodarska-Kowalczyk, M., Pawłowska, J., Zajączkowski, M., 2013. Do foraminifera mirror  
1277 diversity and distribution patterns of macrobenthic fauna in an Arctic glacial fjord?  
1278 *Marine Micropaleontology* 103, 30–39.  
1279 <https://doi.org/10.1016/j.marmicro.2013.07.002>
- 1280 Włodarska-Kowalczyk, M., Pearson, T.H., 2004. Soft-bottom macrobenthic faunal  
1281 associations and factors affecting species distributions in an Arctic glacial fjord  
1282 (Kongsfjord, Spitsbergen). *Polar Biology* 27, 155–167. <https://doi.org/10.1007/s00300->



1283 [003-0568-y](#)

1284 WoRMS Editorial Board, 2019. World Register of Marine Species. Available from  
1285 <http://www.marinespecies.org> at VLIZ. Accessed 2019-05-08.  
1286 <https://doi.org/10.14284/170>

1287 Zaborska, A., Pempkowiak, J., Papucci, C., 2006. Some Sediment Characteristics and  
1288 Sedimentation Rates in an Arctic Fjord (Kongsfjorden, Svalbard). *Ann. Environ. Prot.*,  
1289 8, 79-96.

1290 Zanzerl, H., Dufour, S.C., 2017. The burrowing behavior of symbiotic and asymbiotic  
1291 thyasirid bivalves. *Journal of Conchology* 42, 299–308.

1292

### 1293 **Figures and tables:**

1294 List of tables:

1295 Table 1. Main characteristics of the sampling stations.

1296 Table 2. Bottom water (BW) characteristics for each sampling station:  $C_{org}$ ,  $N_{tot}$ ,  $\delta^{13}C$ ,  $\delta^{15}N$  (in  
1297 %) and C/N values (mean  $\pm$  SD, n=3).

1298 Table 3. Sediment variables for each sampling station: sediment type,  $C_{org}$ ,  $N_{tot}$ ,  $\delta^{13}C$ ,  $\delta^{15}N$ ,  
1299 OM (in %), C/N, Chl *a* ( $\mu g DW g^{-1}$ ) and Chl *a*/Phaeo values (mean  $\pm$  SD, n=no of cores).

1300 Table 4. Functional traits, relative density and biomass of the three dominant taxa for each  
1301 sampling station. Class: P – Polychaeta, B – Bivalvia, An – Anthozoa, As – Asteroidea, O –  
1302 Ophiuroidea, S – Sipunculidea. Mobility and feeding groups (M/F) are marked by codes:  
1303 mobility type (D - Discretely mobile, M – Mobile, S – Sessile) and feeding type (car -  
1304 carnivore, omn - omnivore, sub - subsurface feeder, sur - surface feeder, sus - suspension  
1305 feeder). Burrowing depth (BT): 1 – surface burrowing, 2 – subsurface burrowing, 3 – deep  
1306 burrowing. Tubes (T): “+” – I-shaped tube, “-” – no tube. Sediment mixing types (SMix):  
1307 biodiffusor (B), upward conveyor (UC), gallery diffusor (GD), downward conveyor (DC).

1308 Table 5. PERMANOVA results for the multivariate descriptors of benthic communities with  
1309 significant pair-wise comparisons results for different groups.

1310 Table 6. SIMPER analysis B/D ratio faunal percentage contribution to the average similarity  
1311 for different sampling stations groups. Species that contributed more than 5% are listed.

1312 Table 7. Results of DistLM procedure for fitting environmental variables to the macrofauna  
1313 community data. %Var - percentage of explained variance; %Cum - cumulative percentage  
1314 explained by the added variable. Significance level  $p < 0.05$ . Environmental factors: D –  
1315 depth, S – salinity, T – temperature, types of sediment (mud, sand, gravel), BW  $C_{org}$  – bottom  
1316 water  $C_{org}$ , BW  $N_{tot}$  – bottom water  $N_{tot}$ , BW  $\delta^{13}C$  – bottom water  $\delta^{13}C$  BW, BW  $\delta^{15}N$  –  
1317 bottom water  $\delta^{15}N$ , BW C/N – bottom water C/N, Sed  $C_{org} - C_{org}$  concentration in sediment,  
1318 Sed  $N_{tot}$  – sediment  $N_{tot}$ , Sed  $\delta^{13}C$  – sediment  $\delta^{13}C$ , Sed  $\delta^{15}N$  – sediment  $\delta^{15}N$ , Sed C/N –  
1319 sediment C/N, SOM – sediment organic matter, Chl *a* – sediment Chlorophyll *a* and Chl  
1320 *a/Phaeo* – sediment Phaeopigments.

1321 Table 8. Spearman's rank correlation analyses among biological and physical parameters.  
1322 Significant values are marked in bold ( $p < 0.05$ ).

1323

1324 List of figures:

1325 Fig. 1. Geographical location of the study region (A) and (B) sampling locations during two  
1326 cruises (AX – ARCEX, PS – TRANSSIZ) with two major currents surrounding Svalbard:  
1327 WSC - West Spitsbergen Current, warm Atlantic waters (black) and the ESC – East  
1328 Spitsbergen Current, cold Arctic waters (gray) (after Svendsen et al., 2002).

1329 Fig. 2. Percentages of mobility and feeding groups at different sampling stations. Station ST/8  
1330 marked with \* was sampled in summer season. Functional traits codes: mobility type (D -  
1331 Discretely mobile (yellow), M – Mobile (green), S – Sessile (blue)) and feeding type (car -

1332 carnivore, omn - omnivore, sub - subsurface feeder, sur - surface feeder, sus - suspension  
1333 feeder).

1334 Fig. 3. PCO analysis for macrobenthic communities based on species biomass to density ratio,  
1335 and the Bray-Curtis similarity among four sampling areas: A (Hornsund, Van Mijenfjorden);  
1336 B (Storfjorden); C (Barents Sea shelf); D (northern Barents Sea and Nansen Basin).  
1337 Significantly correlated species with the PCO coordinates ( $r > 0.5$ ) are shown on the plot.

1338 Fig. 4. Mean density (ind./m<sup>2</sup>) (A) and biomass (g/m<sup>2</sup>) (B);  $\pm$  SE, n= no of cores (Table 1) at  
1339 stations sampled in Van Mijenfjorden, Hornsund (group A); Storfjorden (group B); Barents  
1340 Sea shelf (group C); northern Barents Sea and Nansen Basin (group D). Station ST/8 marked  
1341 with \* was sampled in summer season. Kruskal – Wallis results for differences between  
1342 sampling sites are given; significant test results are marked with \*\* ( $p < 0.05$ ).

1343 Fig. 5. Distance-based Redundancy Analysis (dbRDA) plot of the DistLM model visualizing  
1344 the relationships between the environmental parameters and the biomass/density ratio of  
1345 species between four sampling areas: A (Hornsund, Van Mijenfjorden); B (Storfjorden); C  
1346 (Barents Sea shelf); D (northern Barents Sea and Nansen Basin). Environmental variables  
1347 with Pearson rank correlations with dbRDA axes  $> 0.5$  are shown. Environmental factors: D –  
1348 depth, S – salinity, T – temperature, types of sediment (mud, sand, gravel), BW C<sub>org</sub> – bottom  
1349 water C<sub>org</sub>, BW N<sub>tot</sub> – bottom water N<sub>tot</sub>, BW  $\delta^{15}\text{N}$  – bottom water  $\delta^{15}\text{N}$ , BW C/N – bottom  
1350 water C/N, Sed C<sub>org</sub> – C<sub>org</sub> concentration in sediment, Sed  $\delta^{13}\text{C}$  – sediment  $\delta^{13}\text{C}$ , Sed C/N –  
1351 sediment C/N, Chl *a* – sediment Chlorophyll *a* and Chl *a*/Phaeo – sediment Phaeopigments.

1352 Fig. 6. Mean bioturbation coefficients: Db - biodiffusion (cm<sup>2</sup> y<sup>-1</sup>) (A) and r – non-local (y<sup>-1</sup>)  
1353 (B);  $\pm$  SE, n=no of cores (Table 1) at stations sampled in Van Mijenfjorden, Hornsund (group  
1354 A); Storfjorden (group B); Barents Sea shelf (group C); northern Barents Sea and Nansen  
1355 Basin (group D). Station ST/8 marked with \* was sampled in summer season. Kruskal –

1356 Wallis results for differences between sampling sites are given; significant test results are  
1357 marked with \*\* ( $p < 0.05$ ).

ACCEPTED MANUSCRIPT

1358 Appendix 1. Spearman's rank correlation analyses among physical and biogeochemical variables. Significant values are marked in bold ( $p < 0.05$ ).

	Depth	Salinity	Temperature	Gravel	Sand	Mud	BW C <sub>org</sub>	BW N <sub>tot</sub>	BW $\delta^{13}\text{C}$	BW $\delta^{15}\text{N}$	BW C/N	Sed C <sub>org</sub>	Sed N <sub>tot</sub>	Sed $\delta^{13}\text{C}$	Sed $\delta^{15}\text{N}$	Sed C/N	SOM	Chl <i>a</i>	Chl <i>a</i> /Phaeo
Depth	-	<b>0.8</b>	<b>0.8</b>	<b>0.7</b>	-0.2	-0.0	-0.1	<b>0.3</b>	0.1	<b>-0.5</b>	<b>-0.6</b>	<b>-0.6</b>	<b>-0.3</b>	<b>0.4</b>	-0.2	<b>-0.5</b>	<b>-0.4</b>	-0.2	<b>-0.5</b>
Salinity	<b>0.8</b>	-	<b>0.7</b>	<b>0.3</b>	<b>-0.4</b>	<b>0.4</b>	0.2	<b>0.3</b>	-0.0	-0.3	<b>-0.3</b>	-0.2	0.3	<b>0.8</b>	-0.1	<b>-0.5</b>	0.1	0.2	<b>-0.3</b>
Temperature	<b>0.8</b>	<b>0.7</b>	-	<b>0.6</b>	-0.3	-0.0	-0.0	0.1	-0.2	-0.2	<b>-0.3</b>	<b>-0.3</b>	-0.2	<b>0.5</b>	0.0	-0.3	-0.2	-0.1	<b>-0.5</b>
Gravel	<b>0.7</b>	<b>0.3</b>	<b>0.6</b>	-	-0.2	-0.0	-0.1	0.2	<b>0.3</b>	<b>-0.5</b>	<b>-0.6</b>	<b>-0.7</b>	<b>-0.5</b>	-0.0	-0.3	<b>-0.5</b>	<b>-0.7</b>	<b>-0.4</b>	<b>-0.4</b>
Sand	-0.2	<b>-0.4</b>	-0.3	-0.2	-	<b>-0.9</b>	<b>-0.8</b>	<b>-0.7</b>	<b>-0.6</b>	-0.1	0.2	-0.2	<b>-0.5</b>	<b>-0.5</b>	<b>0.5</b>	0.2	-0.2	<b>-0.3</b>	0.0
Mud	-0.0	<b>0.4</b>	-0.0	-0.0	<b>-0.9</b>	-	<b>0.7</b>	<b>0.6</b>	<b>0.6</b>	0.2	0.0	<b>0.3</b>	<b>0.7</b>	<b>0.5</b>	<b>-0.4</b>	<b>-0.3</b>	<b>0.4</b>	<b>0.5</b>	0.1
BW C <sub>org</sub>	-0.1	0.2	-0.0	-0.1	<b>-0.8</b>	<b>0.7</b>	-	<b>0.8</b>	<b>0.6</b>	0.1	-0.2	<b>0.4</b>	<b>0.4</b>	<b>0.4</b>	<b>-0.7</b>	0.2	0.3	<b>0.4</b>	<b>0.3</b>
BW N <sub>tot</sub>	<b>0.3</b>	<b>0.3</b>	0.1	0.2	<b>-0.7</b>	<b>0.6</b>	<b>0.8</b>	-	<b>0.7</b>	<b>-0.4</b>	<b>-0.7</b>	-0.1	0.1	<b>0.4</b>	<b>-0.8</b>	-0.1	0.1	<b>0.4</b>	<b>0.4</b>
BW $\delta^{13}\text{C}$	0.1	-0.0	-0.2	<b>0.3</b>	<b>-0.6</b>	<b>0.6</b>	<b>0.6</b>	<b>0.7</b>	-	-0.1	<b>-0.4</b>	-0.1	0.1	-0.1	<b>-0.5</b>	-0.2	-0.1	0.0	0.1
BW $\delta^{15}\text{N}$	<b>-0.5</b>	-0.3	-0.2	<b>-0.5</b>	-0.1	0.2	0.1	<b>-0.4</b>	-0.1	-	<b>0.8</b>	<b>0.8</b>	<b>0.5</b>	-0.2	<b>0.5</b>	<b>0.5</b>	<b>0.5</b>	-0.2	<b>-0.3</b>
BW C/N	<b>-0.6</b>	<b>-0.3</b>	<b>-0.3</b>	<b>-0.6</b>	0.2	0.0	-0.2	<b>-0.7</b>	<b>-0.4</b>	<b>0.8</b>	-	<b>0.7</b>	<b>0.5</b>	-0.1	<b>0.6</b>	<b>0.3</b>	<b>0.4</b>	-0.0	-0.1
Sed C <sub>org</sub>	<b>-0.6</b>	-0.2	<b>-0.3</b>	<b>-0.7</b>	-0.2	<b>0.3</b>	<b>0.4</b>	-0.1	-0.1	<b>0.8</b>	<b>0.7</b>	-	<b>0.7</b>	0.1	<b>0.3</b>	<b>0.6</b>	<b>0.8</b>	0.1	0.0
Sed N <sub>tot</sub>	<b>-0.3</b>	0.3	-0.2	<b>-0.5</b>	<b>-0.5</b>	<b>0.7</b>	<b>0.4</b>	0.1	0.1	<b>0.5</b>	<b>0.5</b>	<b>0.7</b>	-	<b>0.5</b>	0.2	-0.1	<b>0.8</b>	<b>0.5</b>	0.0
Sed $\delta^{13}\text{C}$	<b>0.4</b>	<b>0.8</b>	<b>0.5</b>	-0.0	<b>-0.5</b>	<b>0.5</b>	<b>0.4</b>	<b>0.4</b>	-0.1	-0.2	-0.1	0.1	<b>0.5</b>	-	-0.2	<b>-0.5</b>	<b>0.3</b>	<b>0.7</b>	0.1
Sed $\delta^{15}\text{N}$	-0.2	-0.1	0.0	-0.3	<b>0.5</b>	<b>-0.4</b>	<b>-0.7</b>	<b>-0.8</b>	<b>-0.5</b>	<b>0.5</b>	<b>0.6</b>	<b>0.3</b>	0.2	-0.2	-	0.2	<b>0.3</b>	<b>-0.4</b>	<b>-0.6</b>
Sed C/N	<b>-0.5</b>	<b>-0.5</b>	-0.3	<b>-0.5</b>	0.2	<b>-0.3</b>	0.2	-0.1	-0.2	<b>0.5</b>	<b>0.3</b>	<b>0.6</b>	-0.1	<b>-0.5</b>	0.2	-	<b>0.3</b>	<b>-0.4</b>	0.0
SOM	<b>-0.4</b>	0.1	-0.2	<b>-0.7</b>	-0.2	<b>0.4</b>	0.3	0.1	-0.1	<b>0.5</b>	<b>0.4</b>	<b>0.8</b>	<b>0.8</b>	<b>0.3</b>	<b>0.3</b>	<b>0.3</b>	-	<b>0.3</b>	-0.0
Chl <i>a</i>	-0.2	0.2	-0.1	<b>-0.4</b>	<b>-0.3</b>	<b>0.5</b>	<b>0.4</b>	<b>0.4</b>	0.0	-0.2	-0.0	0.1	<b>0.5</b>	<b>0.7</b>	<b>-0.4</b>	<b>-0.4</b>	<b>0.3</b>	-	<b>0.7</b>
Chl <i>a</i> /Phaeo	<b>-0.5</b>	<b>-0.3</b>	<b>-0.5</b>	<b>-0.4</b>	0.0	0.1	<b>0.3</b>	<b>0.4</b>	0.1	<b>-0.3</b>	-0.1	0.0	0.0	0.1	<b>-0.6</b>	0.0	-0.0	<b>0.7</b>	-

1359

- This is the first complex report on bioturbation in spring to summer transition conducted over a large depth gradient in the Arctic Ocean.
- Benthic community structure and related biodiffusion and non-local transport varied in Svalbard fjords, Barents Sea and Nansen Basin.
- Changes in environmental conditions, and related changes in quality and quantity of available organic matter, had impact on benthic communities and bioturbation.
- Large inputs of fresh OM to the seabed can trigger bioturbation activities.